SHARE

Grant Agreement no. 226967
Seismic Hazard Harmonization in Europe
Project Acronym: SHARE

SP 1-Cooperation

Collaborative project: Small or medium-scale focused research project

THEME 6: Enviroment

Call: ENV.2008.1.3.1.1 Development of a common methodology and tools to evaluate earthquake hazard in Europe

D4.1– Update strong-ground motion database

Due date of deliverable: 31.06.2010
Actual submission date: 04.06.2010

Start date of project: 2009-06-01   Duration: 36

Middle East Technical University (METU)

E. Yenier, M. A. Sandikkaya, S. Akkar

Revision: 1

Dissemination Level		
PU	Public	x
PP	Restricted to other programme participants (including the Commission Services)	
RE	Restricted to a group specified by the consortium (including the Commission Services)	
CO	Confidential, only for members of the consortium (including the Commission Services)	

**SEISMIC HAZARD
HARMONIZATION IN EUROPE**

**WP4: STRONG GROUND
MOTION MODELLING**

REPORT ON THE FUNDAMENTAL FEATURES
OF THE EXTENDED STRONG-MOTION DATABANK
PREPARED FOR THE SHARE PROJECT

E. Yenier, M.A. Sandıkkaya, and S. Akkar

*Earthquake Engineering Research Center,
Middle East Technical University,
06531 Ankara, Turkey*

February, 2010

TABLE OF CONTENTS

LIST OF TABLES

LIST OF FIGURES

Introduction

This report summarizes the main features of an extended strong ground-motion databank that is compiled within the framework of the "Seismic Hazard Harmonization in Europe" (SHARE) project. The database consists of the accelerograms gathered from the European strong-motion database (ESMD), the Turkish national strong-motion database (T-NSMP), the Next Generation Attenuation database (NGA), the KIK-Net database, the global worldwide database compiled by Cauzzi and Faccioli (C&F), Internet Site for European Strong-motion Data (ISESD) and Italian Accelerometric Archive (ITACA) database. As part of this study, we compare the Turkish and Italian strong-motion sites that are common in local (T-NSMP and ITACA, respectively) and global databases (ESMD, ISESD, NGA and C&F) investigated in this report. The first part of the report describes the major features of each strong-motion databank, identifies their limitations through detailed evaluations and discusses the inconsistencies within or between the databases. These are illustrated by some examples. We also describe our assumptions to handle these deficiencies. This part is followed by the presentation of the database unification methodology to establish the metadata of the global databank. The report finishes by describing the important features of the integrated databank. The discussions in this report define the limitations of the strong-motion databank that will be used in the later stages of WP4 tasks.

Investigated strong-motion databases

(a) Cauzzi and Faccioli (C&F) strong-motion database

The C&F database includes 1163 horizontal and 1131 vertical component records from 60 worldwide earthquakes. These earthquakes are mainly shallow crustal events and are almost exclusively from the USA, Italy, Iceland, Turkey and Japan. The earthquake dates, epicentral locations, earthquake magnitudes, focal depths, source-to-site distances and faulting styles are provided in the database. In terms of source-to-site distance metrics, the epicentral distance (R_{epi}), hypocentral distance[1] (R_{hyp}) and for some records the "*fault*" (closest distance between the station and the rupture surface, R_{rup}) distances are available. Our comparisons between R_{hyp} vs. R_{epi} and R_{hyp} vs. R_{rup} showed two inconsistent cases where R_{hyp} attains smaller values with respect to R_{epi} and R_{rup}. These are kept as they are in the databank because we thought a common decision of the entire group is necessary to remove them from the metadata of the databank. In the last part of the report, we propose a hierarchy for removing the duplicated files in the databank. This procedure can be extended to handle such inconsistent cases.

C&F also provides station codes, station names, station coordinates, mean shear-wave velocities (V_{S30}) and attributed ground conditions (AGC) that is used in defining the soil types in terms of V_{S30} based Eurocode 8 (CEN, 2003) site classification. In their study Cauzzi and Faccioli (2008) used the available V_{S30} information to identify the Eurocode 8 (EC8) site classes. In cases where shear-wave velocity does not extend to 30 m (e.g. some strong-motion stations from K-Net database) the authors used their own procedure that is based on Boore (2004) to approximate fair V_{S30} values. Consequently, the soil types of these strong-motion sites are determined either using the available V_{S30} information or estimations made from above procedure. Site classes that are defined from this methodology (AGC) are generally consistent with the EC8 site classification. However, there are some cases where the attributed site classifications of the authors differ from the EC8 soil classification. These sites are listed in Table A.1 in Appendix A.

---

[1] This distance is abbreviated as "IPO DIST" by Cauzzi and Faccioli. In this report we considered it as the hypocentral distance.

A summary of the outcomes of Table A.1 is also listed in Table 1 in the main text. In brief, a total of 509 sites out of 660 have V_{S30} values in the C&F database. Of the 660 strong-motion sites 616 have AGC information either through V_{S30} or estimated V_{S30} values. The rest of the strong-motion sites do not contain any site class information.

Table 1. Comparisons of the EC8 site categories with those given in the C&F database. The diagonals show the total number of unbiased site classes by C&F since they are consistent with those in the Eurocode 8. Off-diagonals show the total number of conflicting site classes by C&F since they show inconsistency with respect to EC8 soil categories.

		EC8 site class given in C&F			
		A	B	C	D
EC8 site class	A	16			
	B	**8**	221	**5**	
	C		**21**	189	**7**
	D			**1**	39

The instrument models and applied data processing procedures to remove the long-period noise from the raw acelerograms are given as complementary information in the C&F database. In most cases, removing the pre-event mean and acausal high-pass filtering with a 0.05 Hz filter cut-off is applied for removing the long-period noise. Few records are processed by causal filters and one particular ground motion is processed by a tri-linear baseline correction applied to the velocity time series.

We did not detect any inconsistency in the event information: the earthquake names and locations are correctly listed in the C&F database. However, when the station information is of concern, we encountered some inconsistencies. Table 2 shows some examples to this case. Firstly, there are careless mistakes while writing the station names (first two groups in Table 2). In a similar manner, there are minor differences in the coordinates of stations with the same station codes (first group in Table 2). For some cases, the station codes and names are different although the rest of the information exhibits a considerable similarity (third group in Table 2). We note that there is one particular case with conflicting station codes, conflicting station names and conflicting station coordinates. The difference in station coordinates stems from rounding-off the decimals and these stations are assumed as the same. This is presented in last group in Table 2.

Another minor inconsistency is the stations with the same code and name but different station coordinates. We fixed this type of inconsistency by identifying the most frequent station coordinate in the problematic station group. We then used the corresponding station name, station code and coordinate information for that group. (In some cases, rounding-off the decimals in station coordinates results in inconsistent station information as well. For such situations we chose the station with the most precise coordinates in the problematic group). Typical examples of this correction procedure are presented in Table A.2 in Appendix A. Cauzzi and Faccioli stated that most of the observed inconsistencies are related to the erroneous information in the reference databanks that are used during the compilation of their database (personal communication, November 2009).

Table 2 Illustrative cases about the observed inconsistencies in the station information of the C&F database. We used horizontal thin lines to separate the groups that illustrate the problematic cases from each other.

STATION CODE (C&F)	STATION NAME	STATION LAT.	STATION LONG.
515	Pinyon Flat Observatory	33.607	-116.453
515	CA: Pinyon Flat; UCSD Geophys Obs	33.6076	-116.454
534	CA: N Palm Springs; Fire Sta # 36	33.925	-116.548
534	N. Palm Springs Fire Station #36	33.925	-116.548
NCB	Nocera Umbra-Bisc	43.103	12.805
NUB	Nocera Umbra Biscontini	43.103	12.805
593	Tripp Flats	33.602	-116.756
2139	CA: Anza; Tripp Flats Training Camp	33.6022	-116.756

(b) KIK-Net strong-motion database

The database consists of 4704 records from 596 events that occurred in Japan in between 1998 and 2004. The KIK-Net deployed two instruments at each site; one at the surface and the other below the ground so there is a total of 6 components for each recording: 3 at the surface and 3 below the surface. For the particular purposes of this study, we only studied the ground motions recorded at the surface. Each record has a header section containing information about the earthquake, record and the station that includes event time, trigger time, epicentral location, depth, magnitude, station location, epicentral distance, min. / max / average ground acceleration etc. Besides, some response parameters related to the recording instrument and some user defined parameters are also available that are discussed briefly in the below paragraphs. The KIK-Net database is band-pass filtered between 0.25 Hz and 25 Hz (Pousse et al., 2005). The faulting-style information is not presented in the header information.

In addition to the recording files, the database contains supplementary text files with extensions ".info", ".info2", ".txt", "".list_eq", ".list_sta" and ".list_eq_sta". There is another text file with extension ".time_begin_signal" that includes the origin time of the record and the theoretical S-wave arrival time. After examining these files, we observed that most of them duplicate the header information in the recording files. We ascertained this observation by compiling the earthquake, record and station information of the entire database from these files and from the header texts. The comparisons showed no difference. Bearing on this fact; we primarily considered the header information while finalizing the KIK-Net database compilation.

In the original data both the trigger and event times are disseminated in local time. These are converted to GMT during the compilation process. The header information as well as the listed text files above define a number of earthquake magnitude scales without identifying their type. Our investigations on the KIK-Net website resulted in discovering the "user-defined parameter" (user 9) in the header information that defines the JMA magnitude scaling (M_{JMA}) for each event. We used M_{JMA} and converted it to moment magnitude (M_w) using the relation in Pousse et al. (2005) for its use in the metadata.

The source-to-site distance presented in the KIK-Net data is epicentral distance (R_{epi}). We also included the hypocentral distance (R_{hyp}) information calculated by S. Drouet (personnel communication, 2009) as an alternative to R_{epi}. Although we discovered another undefined distance metric in the ".info2" files, we did not incorporate it to the "Main Metadata". Investigation of the distance values resulted in 56 inconsistencies (i.e. $R_{epi} > R_{hyp}$). However, these are mostly due to round-off errors. They are kept as they are as in the case of C&F database.

The KIK-Net data contains recordings from 538 strong-motion sites with well described V_{S30} values. This information is effectively used while classifying the site classes of the data in terms of EC8 and NEHRP soil conditions. We must note that the KIK-Net database also contains some minor discrepancies in the station coordinate and altitude information. We handled this problem in the same way as described for the C&F database. If the problem is related to the conflicting station coordinate information, we identified the most frequent station coordinate from the set of coordinates pertaining to the problematic case and assigned it as the final coordinate. The same procedure is applied for the conflicting altitude information. Appendix B presents a table illustrating typical cases for such stations.

(c) European strong-motion database (ESMD)

This database consists of major earthquakes occurred in and around Europe between 1973 and 2003. The ESMD includes 462 records from 110 events that are obtained from the Volume 2 CD-Rom (Ambraseys et al., 2004a). It is one of the well-detailed global strong-motion datasets and many parameters related to events, records and stations are available in this dataset. Earthquake dates, epicentral coordinates, station locations, depth of events are given. Different earthquake magnitude scales, faulting style and fault solution information is also provided in the database. The estimated fault geometries are used in calculating different distance metrics (R_{epi}, R_{hyp}, R_{JB}[2], R_{rup} etc). Although the database gives information on the fault geometry (strike, dip and slip angles) whenever available, this information is provided for both planes without indicating the correct plane. We note that the database makes point-source assumption for events with $M_w < 5.5$ when fault geometry is unknown. This assumption facilitates the calculations of R_{JB} and R_{rup} for such cases.

If available, the database gives detailed information about the sheltering type of the instruments (structural properties, building type, dimensions etc). A total of 261 stations have EC8 site classes but only 135 of the ESMD sites have V_{S30} values. Detailed site information is given in many of the recording stations (e.g. geologic information, local site conditions etc). All records provided by the ESMD are processed, if available the instrument correction is firstly applied and then acausal Butterworth filtering is used for removing the long-period noise in the record. The filter cut-off frequencies are determined either from the noise in the fixed trace (analog records) or by examining the Fourier acceleration spectra (FAS), and velocity and displacement traces. Although the database contains the calculated strong-motion parameters related to the peak intensities, arias duration, bracketed relative duration etc, these are not considered in the final metadata of this study.

---

[2] Joyner and Boore distance (R_{JB}) is the closest distance measured from the site to the horizontal projection of the fault rupture

When we compared distance metrics relationships among each other, we identified some inconsistencies: $R_{JB} > R_{epi}$, $R_{JB} > R_{hyp}$ and $R_{rup} > R_{hyp}$ for 11, 5 and 7 records, respectively.

(d) Next generation attenuation (NGA) strong-motion database

The database was established by examining the properties of 173 worldwide earthquakes from 1456 sites. A total of 3551 3-component records are available in the NGA database. The event, site and waveform properties are studied in detail. Event related information consists of earthquake dates, epicentral coordinates, if available locations, depths, moment magnitude (almost in all cases), rupture geometries, fault solutions and faulting styles. In addition, a detailed study was performed for the fault modeling of the 63 earthquakes (Chiou et al., 2008). Site characterization is primarily made by V_{S30} according to the NEHRP site classification (BSSC, 2003). Other site classification methods such as Geomatrix, Campbell and Bozorgnia (2003), Bray and Rodriguez-Marek (1997), etc. are also presented in the database. The metadata of NGA database includes information about the instrument type, recording type, building type and various distance metrics (R_{epi}, R_{hyp}, R_{JB}, R_{rup}, Campbell R etc.). Hanging wall indicator and other rupture parameters are also described in this database. The horizontal component definition is GMRotI50 (Boore et al. 2006) in the NGA database but we also preserved the original horizontal components of each accelerogram in order to be compatible with the rest of the databases investigated as they mainly utilize geometric mean (GM) as the horizontal component definition. The bedrock depth information for some recordings is also available in the NGA database and is given in the metadata that is described in the next section of this report. (As part of this study, metadata is uploaded on the Milliarium[3] web site under the WP4 folder).

The waveforms are processed by examining their FAS and displacement traces and by applying either causal or acausal Butterworth band-pass filtering. If this procedure is not adequate (i.e. if the time series still have unexpected variations), the baseline adjustment is applied to the filtered records by subtracting the 2nd time derivative of a polynomial from the acceleration time series that is fitted to the filtered displacement data.

Since the NGA database is one of the well-studied global databases, we could not detect major inconsistencies that might negatively affect the research objectives of the SHARE project. However, the following minor issues are identified while investigating the major features of this database:

- The accelerogram from the Little Skull Mtn, Nv Earthquake that is recorded at the LSM5 station has rupture distance (R_{rup}) greater than the hypocentral distance (R_{hyp}). However, the difference is less than 0.5 km.
- When the record list in the NGA flatfile is compared with the records in hand, firstly, we identified some differences in the record names. We list them in Appendix C.1. We also noted three missing vertical components (Appendix C.2). Finally, some of the records that are listed in the NGA flatfile do not exist in the database (Appendix C.3).
- In addition, we observed that some of the available records have only headers without the acceleration time series (Appendix C.4).

- In the current NGA flatfile some earthquake time information does not exist. We completed some of this missing information from the international seismic agencies.
- For some events, magnitude scales are unknown.
- Of the 1456 strong-motion sites that we traced from the NGA flatfile, we spotted one particular station group that has the same station coordinates and V_{S30} value. These strong-motion sites are listed in Table 3 and we believe that they represent the same strong-motion site.

Table 3 Inconsistencies encountered in terms of station information in the NGA database

STATION CODE (NGA)	STATION NAME	STATION LAT	STATION LONG	V_{S30} (m/s)
839	Kalamata (bsmt)	37.03	22.12	338.6
840	Kalamata (bsmt) (1st trigger)	37.03	22.12	338.6
841	Kalamata (bsmt) (2nd trigger)	37.03	22.12	338.6

(e) Turkish national strong-motion (T-NSMP) database

The recently compiled Turkish strong-motion database gives information on the salient seismological, station and recording parameters that are collected and compiled from the international and national seismic sources (Akkar et al., 2010). The earthquake information gathered for each event in the database consists of the earthquake date, epicentral coordinates, earthquake magnitude in various scales (moment magnitude (M_w), surface-wave magnitude (M_s), body-wave magnitude (m_b), duration magnitude (M_d), and local magnitude (M_L)), depth, and faulting type and solution. In the interest of obtaining more homogenous magnitude information and increasing the number of events associated with moment magnitude values, empirical magnitude-conversion equations were developed relying on the database. The station information for each record involves coordinates, location, ID, altitude and site conditions. The first four parameters were generally obtained from the header information of the records provided by the local seismic agency, GDDA (General Directorate of Disaster affairs). The local site conditions were obtained by conducting field tests. The field tests carried out at each site of interest involved multi-channel analysis of surface waves (MASW), standard penetration test (SPT) and geotechnical laboratory tests (Sandıkkaya, 2008). Borehole seismic tests (BST) were also conducted for some sites to validate the V_S (S-wave velocity) measurements of MASW. The V_{S30} obtained at each strong-motion site through MASW was used for describing the pertaining soil classification.

All records with $M_w \geq 3.5$ are processed for both horizontal and vertical components. The waveform qualities of all records are categorized as specified in Douglas (2003) based on the following five categories of non-standard errors: spike, insufficient digitizer resolution (IDR), multi-event (or multiple shock, MS, events), S-wave triggered (S-WT), early termination during coda (ETDC). The IDR non-standard error is further divided into three categories: moderate, poor and very poor based on the number of levels of acceleration in the records; an objective method suggested by Douglas (2003). Records with non-standard errors of spike, moderate IDR and MS are processed after special treatment but the rest of the records are excluded from the T-NSMP database. After eliminating poor quality records with incurable non-standard problems, accelerograms with $M_w \geq 3.5$ are processed. A bi-directional, fourth-order Butterworth filter is used

during the filtering process. Before starting the actual filtering, an initial baseline adjustment is applied to the accelerograms. If there is a pre-event buffer in the accelerograms (digital records), the mean of 90 percent of this pre-event time is removed from the entire record (i.e. if there is 10 seconds long pre-event time in the record, the average of 9 seconds portion of this was removed from the whole accelerogram). If there is no pre-event information in the acceleration time series (analog records), the mean of the entire record is computed and removed from the entire acceleration time series. The long-period (low-frequency) filter cut-offs for removing the noise in the mean removed accelerograms are estimated in the frequency domain based on the iterative procedure suggested by Akkar and Bommer (2006).

Depending on the level of fault geometry information gathered from the seismic agencies, the R_{JB}, R_{epi}, R_{hyp}, and R_{rup} are calculated. In the case of events whose true rupture locations are sought through special studies, that information was used for the computation of source-to-site distances. For cases where rupture parameters are unknown through the geological and geophysical observations, the concerned variables (i.e. subsurface rupture length, rupture width and rupture area) which are required for the calculation of some of the distance metrics defined above are estimated from the empirical relationships of Wells and Coppersmith (1994).

The faulting styles are primarily determined from the criteria proposed by Frohlich and Apperson (1992) after obtaining the fault plane solutions from the seismic agencies and other sources in the literature. The method of Frohlich and Apperson uses the plunges of P, T and B axes for the fault plane solutions. For cases when these parameters are not provided by the seismic agencies or if the events are classified as "odd[4]" by Frohlich and Apperson, then the rake angle intervals proposed by Boore et al. (1997), Campbell (1997) and Sadigh et al. (1997) are used in the determination of faulting style. In the case of conflicting results between these three methods, the commonly estimated faulting style was accepted as the optimally "correct" style-of-faulting. In order to increase the number of database entries with known fault mechanisms, locations of events were correlated with the locations of known faults.

We selected a total of 1708 (1673 processed + 35[5] unprocessed) T-NSMP records from 755 earthquakes for the purposes of the SHARE project. These strong motions are recorded from 164 sites and 138 of them have V_{S30} values.

(f) Internet Site for European Strong-motion Data (ISESD) database

The Internet Site for European Strong-motion Data (ISESD) database is an internet source that provides strong-motion records from Europe and surrounding countries (Ambraseys et.al, 2004b). The site enables user to search records based on the choices of earthquakes, records or station information (magnitude, site class, epicentral distance, etc).

The parameter and record files contain event date, Flinn Engdahl region, country, epicentral coordinates, depth, magnitudes on different scales, faulting style, station network, country, coordinates, elevation, building type, local geology, V_{S30}, distance

---

[4] The odd style-of-faulting generally refers to oblique faults. The reason T-NSMP did not use this classification is to avoid complex fault descriptions in the database. The user can infer this faulting style definition from the database by using the plunges of P, T and B axes of available fault plane solutions.
[5] The unprocessed records are already used accelerograms in the other databases investigated here. We considered them as part of the T-NSMP database in order to be compatible with the other databases.

metrics (e.g. epicentral and Joyner-Boore distance[6]), source to station azimuth, location and orientation of instrument, instrument type, instrument operator, instrument properties (i.e. sensitivity, natural frequency, damping, full scale amplitude, sampling interval, number of data, resolution of A/D converter, poles of anti-alias filter) and processing scheme.

Instrument correction, as part of strong-motion processing, is applied to the ground-motion records if the necessary information is available. Most of the accelerograms are processed by the 8th order elliptical band-pass filter. The band-pass filter types of a few records are not identified whereas two accelerograms are filtered by the Ormsby band-pass filter. Finally, linear baseline correction is applied to all of the acceleration and velocity time histories.

Events with magnitudes greater than 3 (in any magnitude scale) are selected from the ISESD website by excluding the tremors from mine explosions. A total of 2844 records from 897 events are gathered from this database. These ground motions are recorded by 1079 stations from 34 countries. Table 4 lists the number of downloaded records and corresponding countries. We did not download the whole listed records in the ISESD website because of copyright agreements of strong-motion networks or low waveform qualities. In some cases, the accelerograms are not available despite of their existing names in the ISESD website. This information is also presented in Table 4.

Table 4. Country specific record numbers that are downloaded from the ISESD website and used in the SHARE strong-motion databank.

Country	Number of the records provided in the ISESD	Number of records downloaded from the ISESD website	Number of records included to the SHARE metadata
Albania	5	5	5
Algeria	41	28	28
Armenia	51	38	38
Austria	14	7	7
Bosnia and Herzegovina	19	13	13
Bulgaria	3	3	3
Croatia	29	10	10
Cyprus	4	1	1
Egypt	13	9	9
France	214	28	28
Georgia	188	43	43
Germany	49	31	31
Greece	511	490	490
Hungary	1	1	1
Iceland	400	212	212
Iran	488	396	395
Israel	6	6	6
Italy	1002	593	593

---

[6] This distance metric is indicated as fault distance in the parameter file.

Kyrgystan	5	5	5
Lebanon	1	1	1
Liechtenstein	9	4	4
Macedonia	9	9	9
Norway	11	10	10
Portugal	134	125	125
Romania	35	32	32
Serbia & Montenegro	67	67	67
Slovenia	95	32	32
Spain	282	20	20
Switzerland	148	17	17
Syria	14	10	10
Turkey	634	566	566
United Kingdom	14	3	3
Uzbekistan	31	30	30
Poland(*)	21	21	0
Netherlands(**)	6	0	0
Total	4554	2866	2844

(*) All records are from mine explosions.
(**) None of the records are available.

The site classification of the ISESD database is carried out either by using the shear wave velocity profiles, or the local site geology. A total of 228 sites have V_{S30} values and 442 sites have local site geology descriptions. The remaining sites do not reveal any information on site characterization.

We brought the event date information to a common format and corrected the inconsistent coordinates (e.g. epicenter longitude of the 11/05/1984 10:41:50 Lazio-Abruzzo/Italy aftershock is originally reported as 139208 and it is corrected as 13.9208) during the integration of this database to our metadata. Whenever there are conflicting earthquake and station ID information between the parameter files and accelerogram headers, we preferred the information revealed in the parameter files as they are assumed to contain the most updated data. Two accelerograms from the 28/05/2004 12:38:44 Kojur-Firoozabad, Iran, earthquake have the same station name, station coordinates and acceleration time series. These are considered as the same after the compilation. We also identified a mistake in the station names of two strong-motion sites that are listed in Table 5. The locations of these stations are different as there is considerable difference between their coordinates. Our investigation showed that the first station (in red) in Table 5 is listed with the wrong station name. (We still do not know the actual name of this station). The comparisons of the source-to-station distances given in the ISESD database showed inconsistencies in R_{JB} vs R_{epi} relationships (i.e. $R_{JB} > R_{epi}$) for 67 recordings.

Table 5. Inconsistency in the station names identified during the compilation of the ISESD database. The erroneous station name is shown in red.

STATION ID (ISESD)	STATION NAME	STATION LAT.	STATION LONG.
6264	Mohammad Abad	36.17	53.27
6373	Mohammad Abad	30.88	61.45

(g) Italian Accelerometric Archive (ITACA) database

ITACA project has compiled the strong motion and site class information of the national strong-motion network in Italy. This database is also incorporated in the final metadata of the SHARE project with the collaboration of INGV-Milano team. Milano-INGV strong-motion group provided us the strong-motion waveforms and the corresponding event-, station- and record-related information. This information consists of the following components: event date, location, epicentral coordinates, depth, magnitudes, faulting style, station abbreviation, coordinates, elevation, EC8 site classification, morphological classification, R_{epi}, R_{JB} and R_{hyp} distances, back azimuth, sampling interval, number of data, instrument properties and ground-motion data processing.

ITACA database includes a total of 1165 records obtained from 202 events. Of the entire collection, 156 earthquakes have both moment magnitude and local magnitude information. Number of events with only local or moment magnitude information is 45 and 1, respectively. Faulting style information is available for 150 events.

There are 331 strong-motion stations in the ITACA database. The shear-wave velocity profiles are provided only for 26 stations. The V_S profiles of 22 stations extend up to 30 m whereas they do not reach to 30 m in the rest of the stations. The V_{S30} values of stations with V_S profiles less than 30 m are calculated by extending the shear-wave velocity of the last layer to 30 m. ITACA database presents the estimated EC8 site classes for the remaining sites (i.e. 305 stations)

Analog recordings in the ITACA database are first subjected to instrument correction before any other processing. All strong-motions are processed for baseline shifts. They are then band-pass filtered using a 2nd order acausal Butterworth filter. The procedure followed in band-pass filtering is the one described in Boore (2005). The velocity and displacement time series are examined after the data processing.

Minor inconsistencies that are spotted in the ITACA database are listed in Tables 6 and 7. We observed inconsistencies in epicentral coordinates, magnitudes, depths and faulting styles for 20 events (Table 6). Additionally, the station coordinates of some strong-motion sites are found to be inconsistent (Table 7). These inconsistencies are corrected in the final SHARE strong-motion databank: the most frequent information and/or the coordinate information with the highest precision are taken into account during these corrections.

Table 6. Observed inconsistencies in the event information of the ITACA database. Each group illustrates a particular problematic case. Groups are separated from each other by horizontal lines. The inconsistencies that are shown in red are corrected in the final version of the SHARE strong-motion metadata.

EVENT CODE	EPICENTER LATITUDE	EPICENTER LONGITUDE	DEPTH	M_W	FAULT STYLE
197606081214	46.3	13.23	19.0	4.6	Normal
197606081214	46.3	13.23	19.0	4.6	Undefined
197606171428	46.177	12.798	15.0	4.7	Normal
197606171428	46.177	12.798	15.0	4.7	Undefined
197606261113	46.25	13.11	26.0	4.6	Normal
197606261113	46.25	13.11	26.0	4.6	Undefined
197609071108	46.3	12.983	5.0	4.2	Normal
197609071108	46.3	12.983	5.0	4.2	Undefined
197609111631	46.29	13.18	10.0	5.1	Reverse
197609111631	46.29	13.18	10.0	5.1	Undefined
197609150438	46.267	13.167	21.0	4.9	Normal
197609150438	46.267	13.167	21.0	4.9	Undefined
197609150458	46.267	13.167	19.0	4.6	Undefined
197609150458	46.3	13.15	19.0	4.6	Undefined
199804051552	43.1897	12.7673	4.4	4.8	Normal
199804051552	43.19	2.773	5.4	4.7	Normal
200904060132	42.33	13.33	8.8	6.3	Normal
200904060132	42.334	13.334	8.8	6.3	Normal
200904060237	42.37	13.34	10.1	5.1	Normal
200904060237	42.366	13.34	10.1	5.1	Normal
200904062315	42.45	13.36	8.6	5.1	Normal
200904062315	42.451	13.364	8.6	5.1	Normal
200904070926	42.34	13.34	10.2	5	Normal
200904070926	42.342	13.338	10.2	5	Normal
200904071747	42.27	13.46	15.1	5.6	Normal
200904071747	42.275	13.464	15.1	5.6	Normal
200904072134	42.38	13.38	7.4	4.6	Normal
200904072134	42.38	13.376	7.4	4.6	Normal
200904082256	42.51	13.36	10.2	4.1	Normal
200904082256	42.507	13.364	10.2	4.1	Normal
200904090052	42.48	13.34	15.4	5.4	Normal
200904090052	42.484	13.343	15.4	5.4	Normal
200904090314	42.34	13.44	18.0	4.4	Normal
200904090314	42.338	13.437	18.0	4.4	Normal
200904090432	42.45	13.42	8.1	4.2	Normal
200904090432	42.445	13.42	8.1	4.2	Normal
200904091938	42.5	13.36	17.2	5.3	Normal
200904091938	42.501	13.356	17.2	5.3	Normal

200904132114	42.5	13.36	7.5	5.1	Normal
200904132114	42.504	13.363	7.5	5.1	Normal

Table 7. Observed inconsistencies in the station coordinates of the ITACA database. Each group illustrates a particular problematic case and the groups are separated from each other by horizontal lines. The inconsistencies that are shown in red are corrected in the final version of the SHARE strong-motion metadata.

STATION CODE	STATION LATITUDE	STATION LONGITUDE
BOJ	41.484451	14.472103
BOJ	41.484500	14.472100
CAG	43.054400	12.828900
CAG	43.054000	12.829000
NCR	43.111583	12.784666
NCR	43.111600	12.784700
PIC	42.850376	11.684975
PIC	42.850400	11.685000
SCP	41.807213	15.164646
SCP	41.807200	15.164600
SNM	43.934326	12.449290
SNM	43.934300	12.449300
SNS	43.567390	12.143375
SNS	43.567400	12.143400
TMO	41.989445	14.975007
TMO	41.989400	14.975000

When we compared the source-to-station distances in the ITACA database we observed inconsistencies between different distance relationships (i.e. $R_{JB} > R_{epi}$ and $R_{JB} > R_{rup}$ for 192 and 18 records, respectively). The discrepancies between these distance metrics are less than 0.5 km for the majority of inconsistent cases and they are kept as they are for the final decision of the WP4 group as in the case of other similar inconsistencies spotted in this study.

(h) Details of site class information collected from the ITACA and T-NSMP databases

As stated previously, the ITACA and Turkish National strong-motion projects have compiled the strong motion and site class information of the national strong-motion networks in Italy and Turkey, respectively. We used the site class information disseminated by these databases to compare the Italian and Turkish strong-motion site classifications in the C&F, NGA, ESMD and ISESD databases. Tables D1 to D4 list the conflicting site class information between ITACA and the aforementioned strong-motion databases in terms of EC8 site classification. Tables D5 to D8 provide a similar comparison for T-NSMP.

Table 8 summarizes the seismological parameters, recording and station information disseminated by the strong-motion databases investigated within the scope of this report.

Table 8. Main features of the strong-motion databases investigated

	C&F	KIK-Net	ESMD	NGA	TNSMP	ISESD	ITACA
Earthquake date and time	x	x	x	x	x	x	x
Epicenter coordinates	x	x	x	x	x	x	x
Focal depth	x	x	x	x	x	x	x
M_w	x	x[1]	x	x	x	x	x
M_d			x		x		
M_s			x	x	x	x	
M_b			x		x	x	
M_L			x	x	x	x	x
Fault modeling and rupture parameters				x			
Fault dimensions				x	x		
Fault solutions			x	x	x		x
Faulting style	x		x	x	x	x	x
Station coordinates	x	x	x	x	x	x	x
Station name	x		x	x	x	x	x
R_{epi}	x	x	x	x	x	x	x
R_{hyp}	x	x	x	x	x		x
R_{JB}			x	x	x	x	x
R_{rup}	x		x	x	x		
Hanging wall parameters				x			
V_{s30}	x	x	x	x	x	x	x
Site class (not from V_{S30})	x		x	x		x	x
Depth to basement rock				x			
Z1.0				x			
Z1.5				x			
Z2.5				x			
Geological information			x	x		x	x
Instrument model	x		x	x	x	x	x
Recording type		x		x	x		x
Structural properties of instrument shelter			x	x	x		
Data processing parameters	x	x	x	x	x	x	x

[1] converted from M_{JMA}

13

Unification of the strong-motion databases

The limitations of each database that is discussed in the previous section are considered carefully while gathering the metadata of the SHARE databank together. The unification methodology follows the steps described below:

1. Number the rows of each database with a specific code,(termed as GM-CODE),
2. Give a code to each earthquake in the databases. This code is actually in the form of yyyymmddhhmm, (termed as EQ-CODE),
3. Paste the GM-CODE and EQ-CODE to the first two columns of the metafile
4. Start transferring the information from each database to the metafile in a columnwise manner,
5. Collect similar type of information from different databases under the same column heading,
6. After transferring all the relevant information to the metafile start identifying the duplicated "*events*" from different databases:
   a. Sort the metafile by EQ-CODE and identify the earthquakes with approximately the same date and time.
   b. Sort the above identified event (candidates for duplicated earthquakes) by epicentral coordinates.
   c. Give higher weights to the above events from different databases using the below arguments
      i. if they have almost the same time and epicentral location
      ii. if they have almost the same magnitude and faulting style
      iii. if they have almost the same depth (optional, if and only if the depth information is reliable)
      iv. if there exists common recording stations
   d. Based on the total weights collected from the above arguments, use the expert judgment to identify the duplicated "*events*" (higher the total weights is higher the probability of being a duplicated event)
7. For a pre-identified duplicated "*event*", specify the duplicated "*records*" using the following arguments:
   a. Sort the records of the duplicated event by station coordinates
   b. Give higher weights to these sorted records
      i. if they have almost the same station coordinates
      ii. if they have almost the same station name
      iii. if they have almost the same V_{S30}
      iv. if they have almost the same epicentral distances
      v. if they have almost the same PGA values (optional, because causal/acausal filtering makes a great difference even for the horizontal component PGA values – see discussions by DM Boore on the "unpublished notes" section of his website –)
      vi. if they have the same recording instrument (optional, if and only if the instrument information is reliable)
   c. Based on the total weights collected from the above arguments, use the expert judgment to identify the duplicated "*records*" (higher the total weights is higher the probability of being a duplicated record)
8. Steps 6 and 7 also spot the duplicated stations of different databases. This way these are also identified in the final metafile.
9. After filtering out the duplicated events, records and stations, the rest of the metafile is recoded for new event, record and station indices. (Note: filtering out these records does not correspond to removing them from the metafile. They are not considered in the new indexing).

14

A total of 248 events, 505 stations and 983 records are identified as duplicated during the unification procedure. These are presented in the metafile of the strong-motion databank with the same event, station and waveform id numbers. The metafile is decomposed into 6 separate sheets. The first sheet is called as "Main Metadata" and it includes the major features of the events (event ID, event date, epicentral coordinate, depth, magnitude, fault dimensions, faulting style and fault solutions), station information (station ID, station name, station coordinates, station location, altitude, site-to-source distances, V_{S30} values, V_{S30} origin –measured/inferred-, site classes, local site and geological information) and recording information (record ID, recording instrument, recording type, shelter type, recording name, orientation of instrument, peak ground motion amplitudes, filtering technique, data processing parameters, and usable period). The other sheets describe the specific seismological features presented by each investigated strong-motion database.

Important Features of the Integrated Databank

The unified metafile is discussed in terms of various seismological parameters to present the general characteristics of the integrated databank. This way one can have a general overview about the extents of the databank for accomplishing the relevant objectives of the SHARE project. The databank covers earthquakes back to 1930s and contains a total of 2448 events (Figure 1) and 14193 records. As previously mentioned, the unified metafile currently includes replica of some earthquakes, stations and records. During the evaluation of unified SHARE strong-motion databank, the duplications are not considered. This is performed by establishing a hierarchy in which the highest priority is given to the information gathered from the local databases (i.e. T-NSMP for Turkish data, KIK-Net for Japanese data and ITACA for Italian data) that is followed by ESMD and ISESD for the European data, and NGA and C&F for the worldwide data, respectively. No hierarchy is established between the local databases because they do not contain overlapping events, stations or recordings. Note that the C&F database is a collection of ground-motion data from earlier versions of various sources (personnel communication with Cauzi and Faccioli, 2009). Therefore, ESMD, ISESD and NGA databases that include more recent information are given higher priority with respect to the C&F database.

The assessment of the unified databank is performed in terms of moment magnitude (M_w), focal depth, faulting style, EC8 site category, source-to-site distances, filter cut-off frequencies and usable period ranges of the ground-motion records. The hierarchy is applied separately to the first four parameters in order to the select the representative data from duplications.

The unified databank presents EC8 site categories determined either from V_{S30} or overall geological settings that are used by the reference databases. While selecting the EC8 site classes of duplicated stations, the ones based on V_{S30} are given higher priority. The above hierarchy is implemented when the V_{S30} information is available from multiple databases. This is also the case for site classes that are determined from geological settings. In other words, we considered the same hierarchy as described above when there is more than one database giving the geology-based site class information for the duplicated station. We followed the same hierarchy for defining the source-to-site distances when the duplicated records are of concern. The hierarchy is proceeded such that the entire set of distance metrics is considered from the "chosen" database in order to avoid possible inconsistencies between the distance metrics (e.g. $R_{epi} > R_{hyp}$, $R_{JB} > R_{epi}$ or $R_{rup} > R_{hyp}$).
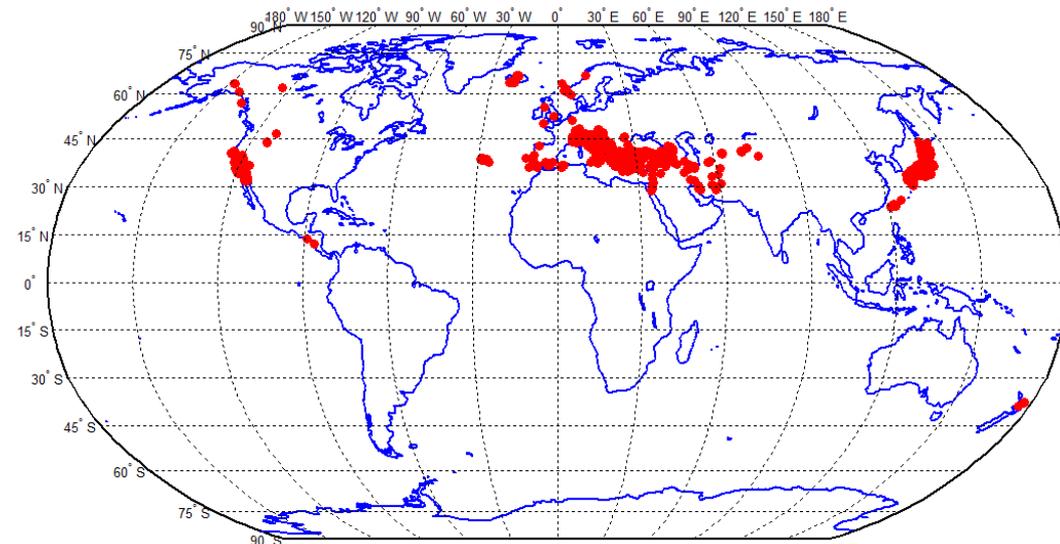
Figure 1. Epicenter locations of the earthquakes presented in the unified databank

Figure 2 demonstrates the yearly basis distribution of the earthquakes and ground-motion records given in the unified databank. About 50% of the events in the databank occurred in the last decade. Again, more than 50% of the ground-motion records belong to this time span. Higher concentration of the events and records in the last ten years can be attributed to the increased number in recording instruments all around world. Another important conclusion from this statistics is the dominancy of digital recordings in the database as significant number of digital sensors has been deployed in the seismic prone regions during the last decades.
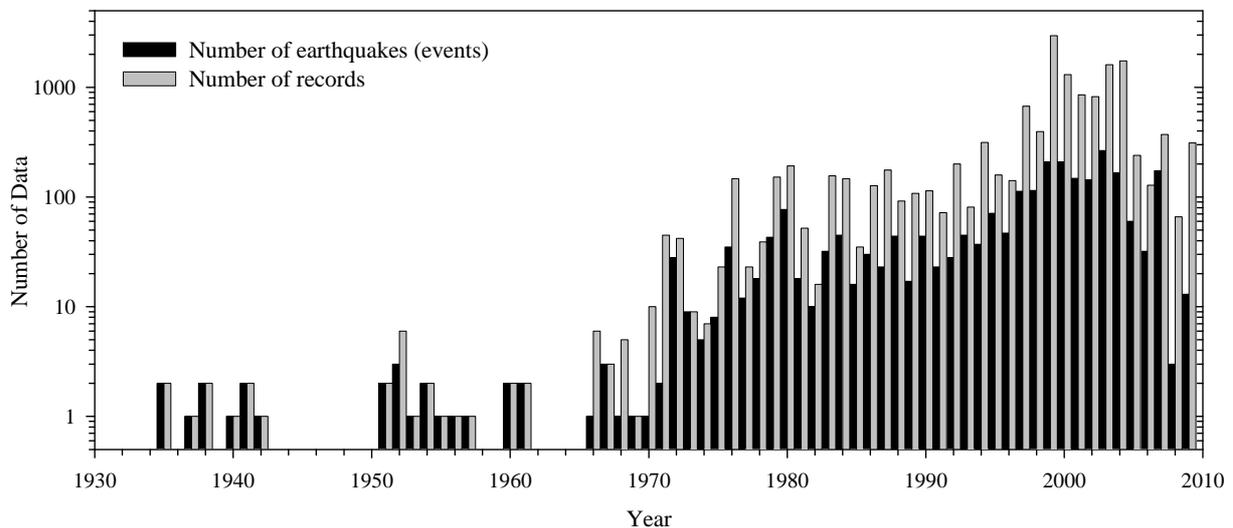
Figure 2. Yearly basis histogram of the earthquakes and ground-motion records existing in the integrated databank. Note that vertical axis is presented in log-scale for a better visual inspection.

16

Figure 3 shows the histograms that display the distributions of some of the important seismological parameters in the databank. Most of the events (1879 events out of 2448) are reported in terms of moment magnitude (M_w) and the majority of these events have magnitudes $M_w \leq 5.0$. The fraction of events that can be considered as large earthquakes (i.e. $M_w \geq 6.5$) constitutes only 2.5% of the entire databank. When the focal depth is of concern, Figure 3.b indicates that the databank dominantly consists of shallow crustal earthquakes (about 84% of the entire databank has focal depths less than 20 km). The faulting style distribution that is displayed in Figure 3.c shows that many events (mostly the small magnitudes) lack mechanism solution. This deficiency can be prevailed by overlying these events on the relevant seismotectonic maps to judge the faulting styles of some of them that are close to the well-known faulting zones. Among those with known faulting styles the majority of the events are strike-slip and this is followed by the dip-slip faults with dominant normal and reverse components, respectively. The faulting styles of few events are identified as oblique without dominant slip components.

Figure 4 displays similar types of histograms as in Figure 3 but exhibits the distributions for number of accelerograms. The record distribution as a function of M_w (Figure 4.a) displays a better variation when compared to the same distribution for number of events (Figure 3.a). This observation shows the fact that in spite of the small number of large magnitude earthquakes, the recorded number of strong-motions from these events is significant. The comments on the depth distribution of records are similar to those given in Figure 3.b: most of the recordings are from shallow crustal earthquakes. The distribution of records in terms of faulting style also exhibits approximately the same information as in the case of Figure 3. The major fraction of strong-motion records is from the events of unknown faulting styles and few records fall into the oblique faulting category. We note that the number of strike-slip and reverse accelerograms are almost the same and constitute a larger group with respect to the normal style records. The final histogram presented in Figure 4 shows the distribution of databank in terms of site classification of EC8. The majority of the sites can be considered as dense-to-stiff site classes (B and C sites). The rock sites ($V_{S30} > 800$ m/s) constitute approximately the 10% of the entire databank whereas recordings from EC8 D sites represent 2% of the database. There are only 4 records from EC8 E sites in the unified databank. Also note that site categories of more than 1000 ground motions are unknown.
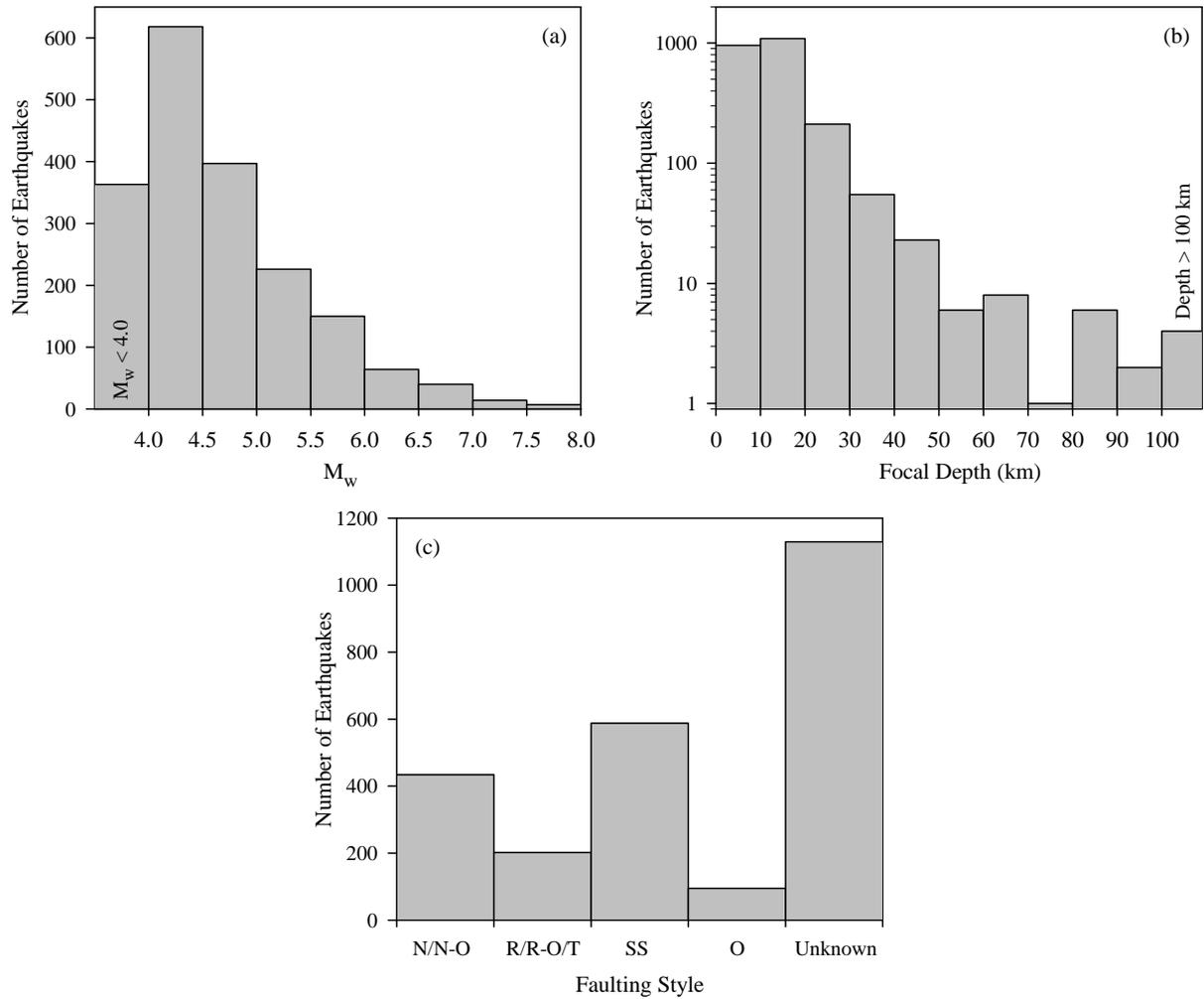
Figure 3. Event histograms in terms of (a) moment magnitude, M_w, (b) focal depth, (c) faulting style distribution. The abbreviations used in the faulting style histogram are as follows: N is normal, N-O is normal-oblique, R is reverse, R-O is reverse-oblique, T is thrust, SS is strike-slip and O is oblique.
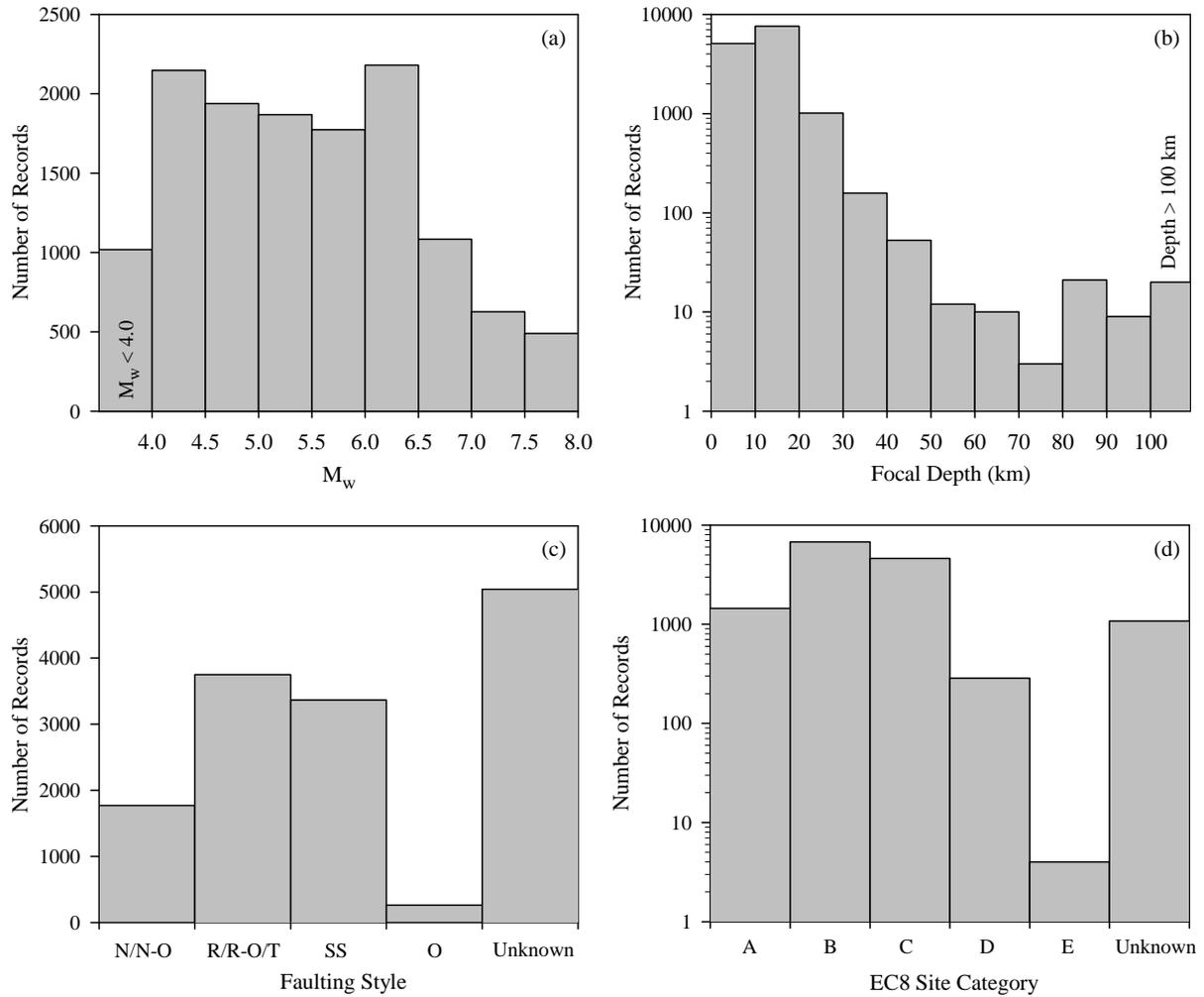
Figure 4. Histograms of ground motions in the metadata for (a) moment magnitude, M_w, (b) focal depth, (c) faulting style and (d) EC8 site classification. The faulting style abbreviations are already given in the caption of Figure 3. The V_{S30} ranges of EC8 site definitions are A: $V_{S30} > 800$ m/s, B: 360 m/s $\leq V_{S30} \leq 800$ m/s, C: 180 m/s $\leq V_{S30} < 360$ m/s and D: $V_{S30} < 180$ m/s. EC8 E is defined as a special site category where the soil profile consists of a surface alluvium layer with V_S values of EC8 C or D and thickness varying between about 5-20 m, underlain by stiffer material with $V_S > 800$ m/s.

The moment magnitude vs. source-to-station distance scatters are presented in Figure 5. The distance metrics are R_{epi}, R_{hyp}, R_{JB} and R_{rup}. The latter two distance metrics are widely used in the current predictive models. Figures 5.a and 5.b are plotted in terms of R_{epi} and R_{hyp}, respectively. Since the calculation of these distance metrics is relatively easier than R_{JB} and R_{rup}, the pertaining scatter diagrams show abundant number of data (more than 11,000 recordings have R_{epi} and R_{hyp} distance information). The number of data in the SHARE databank reduces significantly if we only account for the direct information of R_{JB} and R_{rup}. For these cases the number of usable records is approximately 5,700 and 4,400 for R_{JB} and R_{rup}, respectively. Their M_w vs. R_{JB} and M_w vs. R_{rup} scatter points are shown in blue in Figures 5.c and 5.d. As in many applications, one can use point-source assumption for small magnitude events (i.e. $R_{JB} \approx R_{epi}$ and $R_{rup} \approx R_{hyp}$ for $M_w < 5.0$) in order to increase the number of data with R_{JB} and R_{rup} information. Under such an assumption an additional ~3,700 records can be considered in Figures 5.c and 5.d that are shown as red scatter points. (In order to verify point-source assumption for $R_{JB} \approx R_{epi}$ and $R_{rup} \approx R_{hyp}$ in small

19

magnitude events, we refer to the scatter plots in Figure 6. They are plotted using the metadata to show the variations of R_{JB} vs. R_{epi} and R_{rup} vs. R_{hyp} for different magnitude ranges. It is clear that for the smallest magnitude range the above assumption is valid particularly when the distances attain large values). We note that the differences in the definitions of these distance metrics result in variations in the distance bounds for each case. For M_w vs. R_{epi}, the data possesses a more uniform distribution for $R_{epi} \geq 5$ km whereas this limit shifts to $R_{hyp} \geq 10$ km in Figure 5.b. The R_{JB} displays a better data distribution with respect to R_{rup} particularly after the implementation of point-source assumption ($R_{JB} \approx R_{epi}$ when $M_w < 5.0$). For this case the data distribution can be accepted as uniform for R_{JB} values greater than 0.5 km. Note that the uniformity of metadata loosens with decreasing magnitude when the concerned distance metric is R_{rup}.
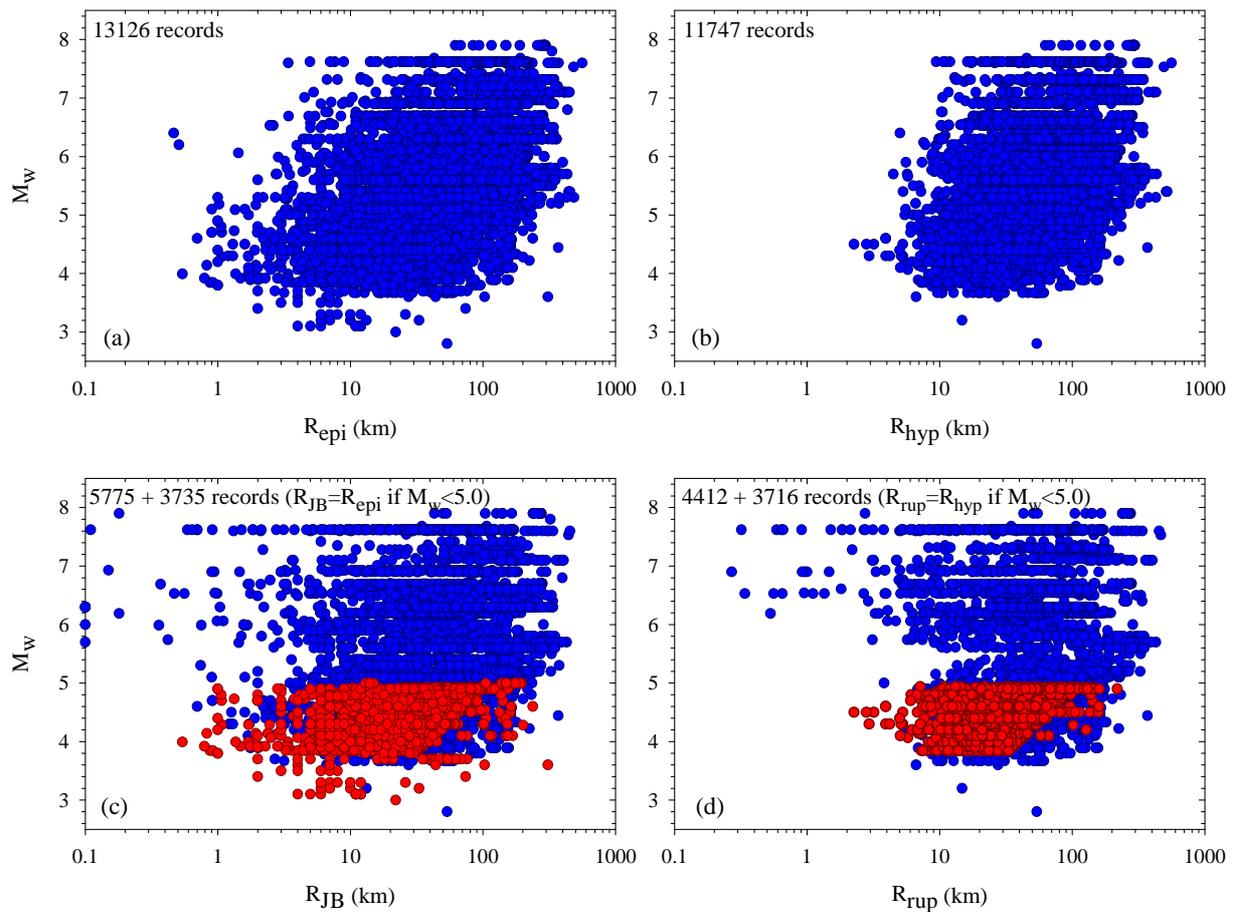
Figure 5. Distribution of unified databank in terms of M_w and (a) epicentral distance, R_{epi}, (b) hypocentral distance, R_{hyp}, (c) Joyner and Boore distance, R_{JB} and (d) rupture distance, R_{rup}. The records with $R_{JB} \approx R_{epi}$ and $R_{rup} \approx R_{hyp}$ assumptions for $M_w < 5.0$ are shown as red scatters in Figures 5.c and 5.d. The total number of records for each magnitude-distance bin is given on the upper-left corner in each plot.
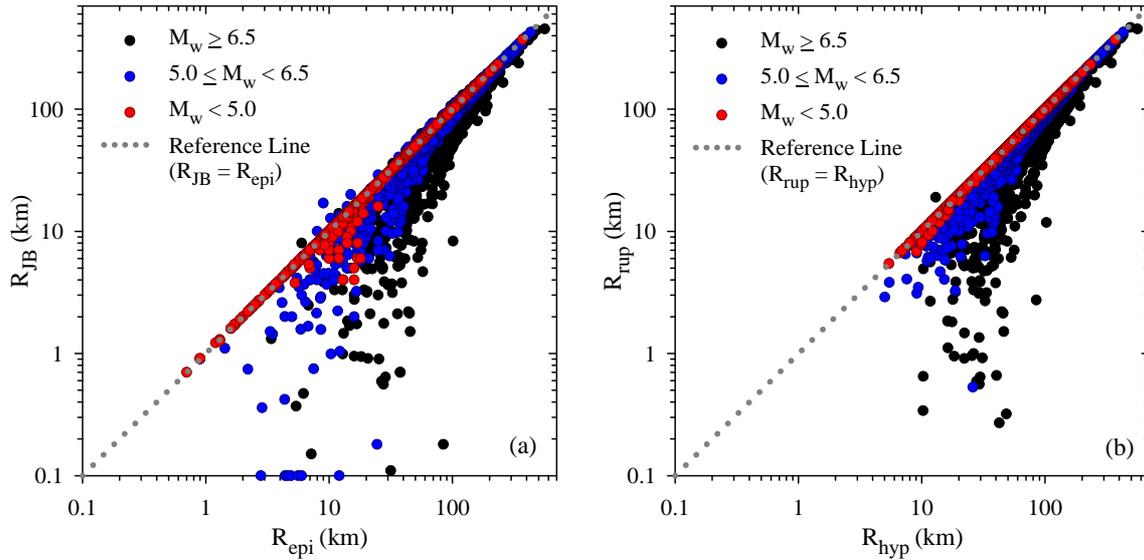
Figure 6. Magnitude-dependent empirical (a) R_{JB} vs. R_{epi} and (b) R_{rup} vs. R_{hyp} scatters plotted from the unified SHARE databank. As previously stated, the distance values reported by some reference databases show inconsistencies (i.e. $R_{JB} > R_{epi}$ and $R_{rup} > R_{hyp}$) for some records. The distance scatters of these records are shown above the reference line.

The M_w-R_{rup} distribution in Figure 5.d is repotted as a set of scatter plots in Figure 7 for different faulting mechanisms. The plots include the additional records due to point-source assumption for M_w < 5.0. The scatters also display information about the total number of earthquakes and records for each faulting-style. The magnitude vs. distance distribution of strike-slip records shows higher resolution with respect to the other faulting-style bins. Strike-slip records are followed by the normal and reverse records. The records with normal slip (or predominantly dipping in the normal direction) display a good distribution for 3.5 < M_w ≤ 7.0 and 5 km < R_{rup} < 200 km. Reverse records (or those with predominant reverse slip components) show a more dispersive behavior. There is a lack of recordings between 5.0 < M_w < 5.5 for this faulting style. Figure 7.d shows the M_w vs. R_{rup} distribution of accelerograms with oblique faulting style and those without an attributed mechanism. Most of the ground motions of unknown faulting mechanisms have M_w < 5.0. About 95% of the records without faulting style information pertain to the KIK-Net database.
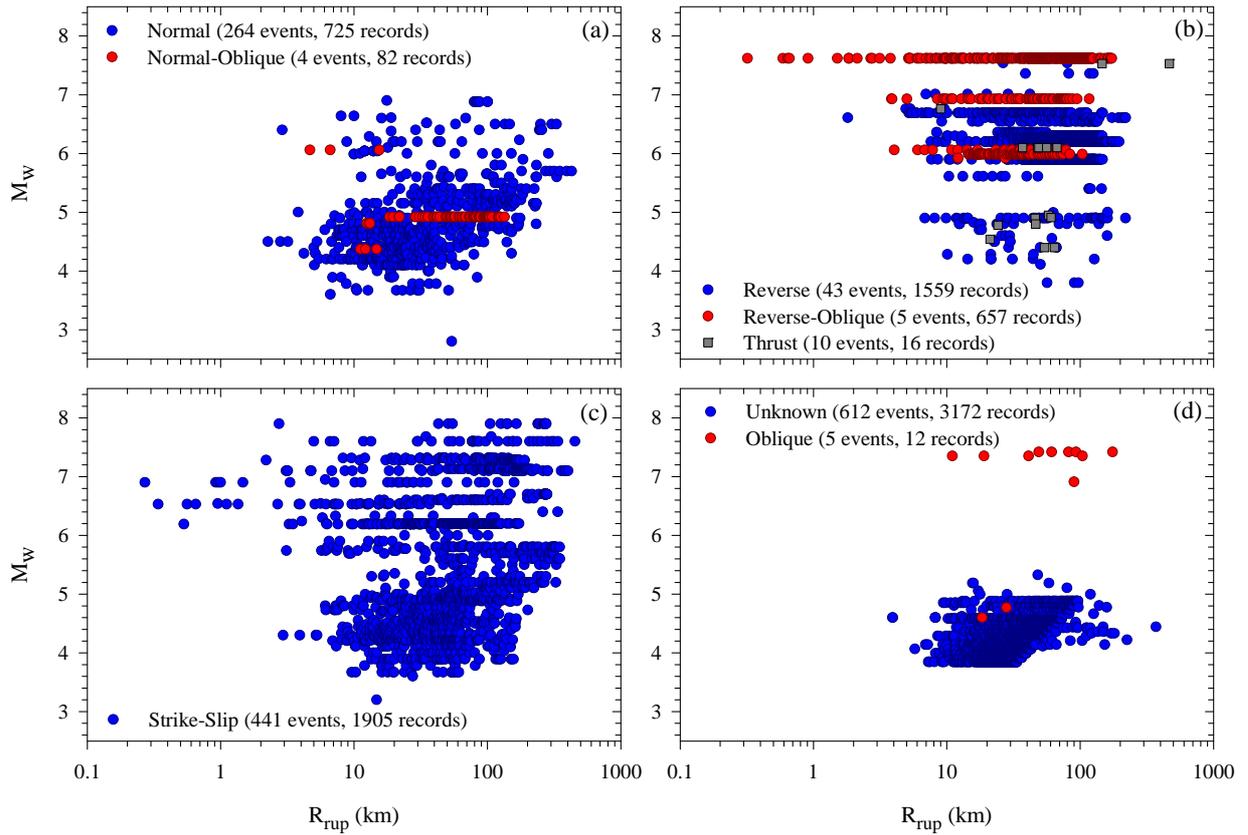
Figure 7. M_w-R_{rup} scatters of ground motions as a function of faulting styles: (a) Normal faulting (b) Reverse faulting (c) Strike-slip faulting (d) Unknown and oblique faulting. The ranges of horizontal and vertical axes are kept same for each scatter due to comparative purposes.

Figure 8 illustrates the M_w-R_{rup} distribution of the ground-motion records in terms of EC8 site categories. The EC8 site categories are based on V_{S30} values if V_{S30} information is available. For sites without V_{S30} information, the estimated EC8 site categories reported by reference databases are used. It can be directly inferred that the unified SHARE databank is dominated by the ground motions recorded at B and C sites that is already discussed in Figure 4. These site classes are followed by site class A and site class D records, respectively. Note that the poorest M_w-R_{rup} distribution pertains to D site class ground motions. The site class A records are grouped into two separate magnitude ranges with a lack of data between $5.0 < M_w < 6.0$. This gap is also observed for site class D records (Figure 8.d). The site class D records are loosely distributed between 10 km $< R_{rup} <$ 200 km with a shift towards larger distances for large magnitude records. The M_w-R_{rup} variations of EC8 B and C ground motions have similar distributions for $3.5 < M_w < 8.0$ and $R_{rup} > 10$ km (Figures 8.b and 8.c). Regardless of the site classification the M_w-R_{rup} distribution is poor for $M_w < 6$ and $R_{rup} < 10$ km. Note that this observation is specific to M_w-R_{rup} distribution of the databank. The same limitation would not be observed for M_w-R_{JB} variation.

Figure 9 shows the M_w-R_{rup} distribution of the ground motions with unknown site classes. Almost all records are in between $4.0 < M_w < 6.0$ and their distances are mainly distributed between 10 km $< R_{rup} <$ 100 km. Identification of their site classes will improve the M_w vs. R_{rup} distributions in particular if they pertain to A and D site categories.

22
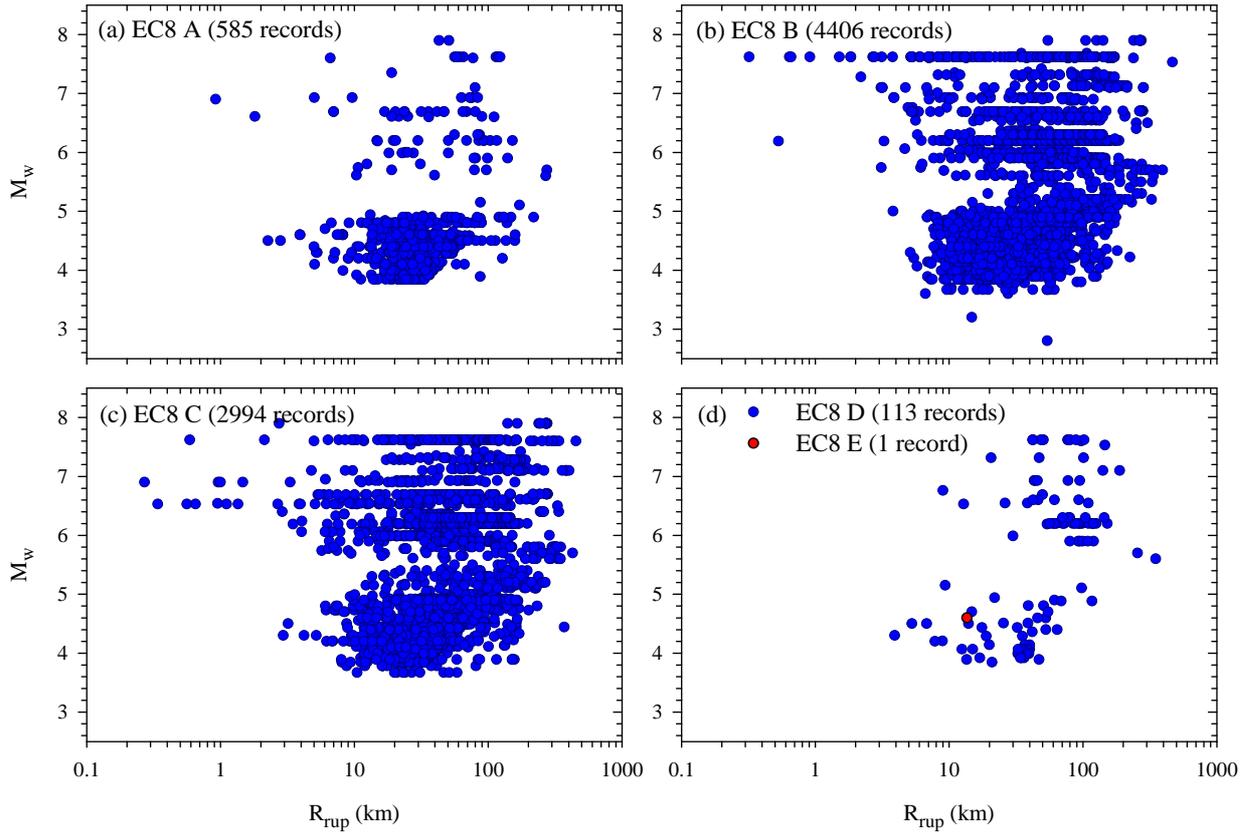
Figure 8. M_w-R_{rup} scatters of ground motions in terms of EC8 site classification. The scatters also contain the additional records obtained from the point-source assumption ($R_{rup} \approx R_{hyp}$ for $M_w < 5.0$). The total number of records in each site class is given on the upper left corner of the scatter panels.
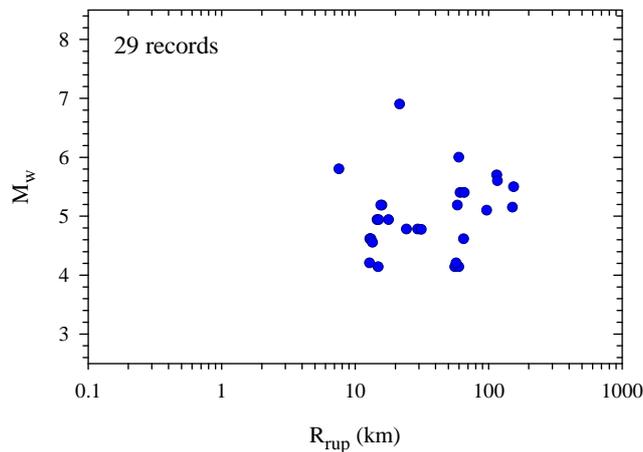
Figure 9. M_w-R_{rup} scatters of ground motions without EC8 site category

The comparison of high-pass (low-cut) filter cut-offs with respect to the theoretical source-spectrum corner frequencies is useful for evaluating the reliability of processed ground-motion parameters. If the chosen filter cut-off frequency ($f_{low-cut}$) is greater than the theoretical corner frequency of source spectrum, some portion of the actual frequency content is most

likely removed. The chosen $f_{low-cut}$ values of the processed horizontal components in the databank are assessed by using the theoretical double-corner source-spectrum corner frequencies proposed by Atkinson and Silva (2000). This is illustrated in Figure 10. The distribution of $f_{low-cut}$ with respect to M_w for different site conditions indicates that most of the $f_{low-cut}$ values are smaller than f_{AS00-I} (corner frequency that controls the total rupture area and strong-motion duration). There are considerable number of records with $f_{low-cut}$ values between f_{AS00-I} and $f_{AS00-II}$. For soft and stiff sites when moment magnitude takes values larger than 6.0, the chosen flow-cut values of some records seem to be significantly higher than the theoretical source-spectrum corner frequency f_{AS00-I}. For these cases, one may infer that the record is subjected to excessive low-cut filtering and its long-period components are distorted after data processing.
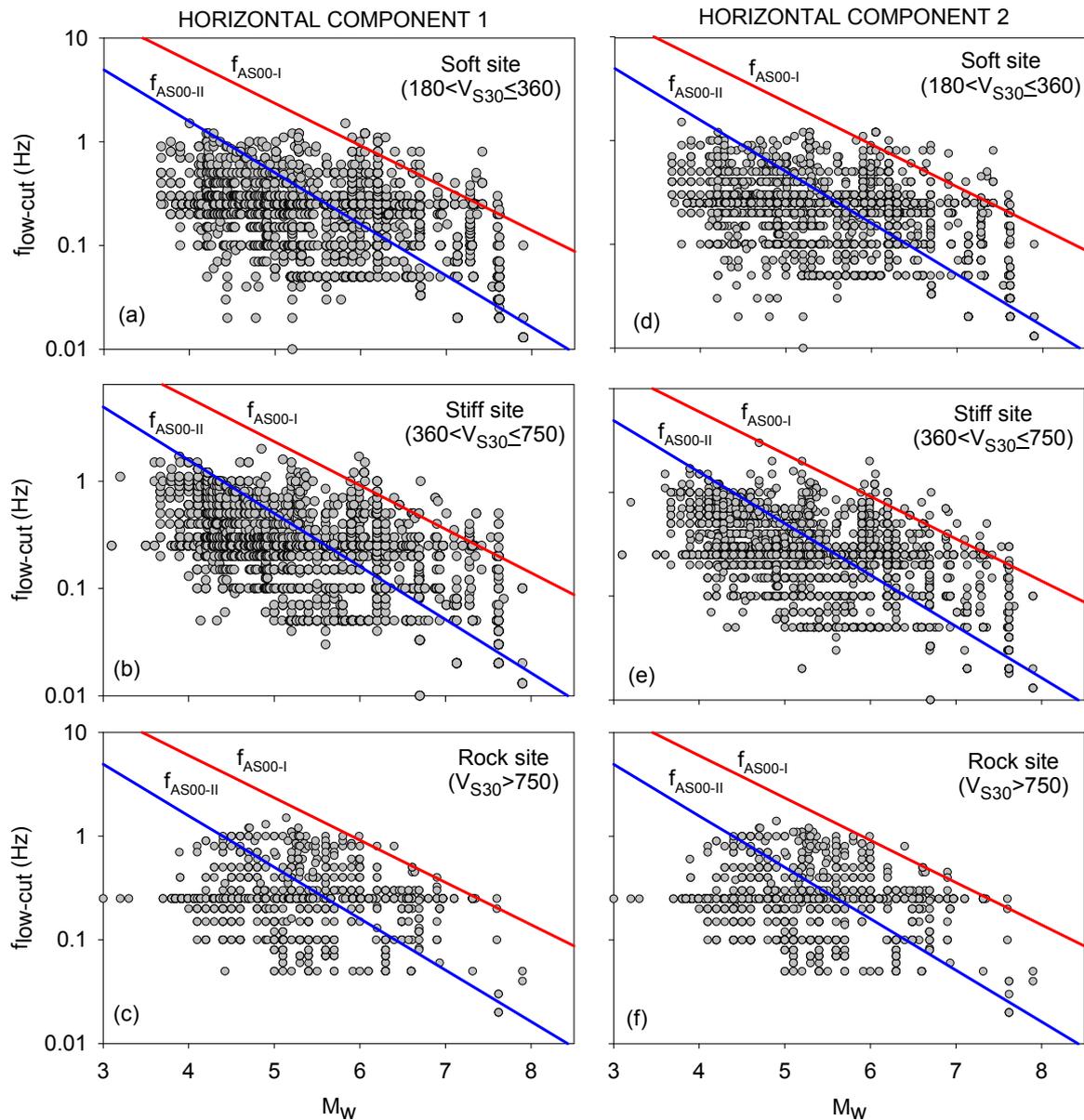
Figure 10. The distributions of the $f_{low-cut}$ with respect to M_w for soft (top row), stiff (middle row) and rock (bottom row) sites. The scatters for horizontal components are displayed column-wise.

We also investigated the usable period range of the horizontal components in the SHARE databank by using the procedure proposed in Akkar and Bommer (2006). This empirical procedure makes use the low-cut filter period (T_c, reciprocal of $f_{low-cut}$) and modifies it with some certain constants to determine the usable period range of each recording as a function of site class and recording type (i.e. analog vs. digital). Accordingly, for analog instruments, the usable period for rock, stiff and soft sites is bounded by $0.65T_c$, $0.70T_c$ and $0.70T_c$, respectively. For digital instruments, the usable period is bounded by $0.80T_c$, $0.90T_c$ and $0.97T_c$ for rock, stiff and soft sites, respectively. Figure 11 shows the variations in the number of recordings with respect to the usable periods calculated by Akkar and Boomer (2006). It is observed that the number of data decreases with increasing oscillator period (T). There is a sudden jump towards lower values in the digital data for T > 3.0s because the KIK-Net data are removed almost entirely from the databank since they are low-cut filtered with a constant value of T_c = 4.0s regardless of the variations in their frequency content. The magnitude-distance-site class scatters of the usable SHARE databank at different vibration periods are illustrated in Figure 12. Inherently, regardless of the site class, the number of data decreases significantly with increasing T, especially for T $\geq$ 5.0s. It is also noted that the number of data is very limited for rock sites, especially for T $\geq$ 5.0s.
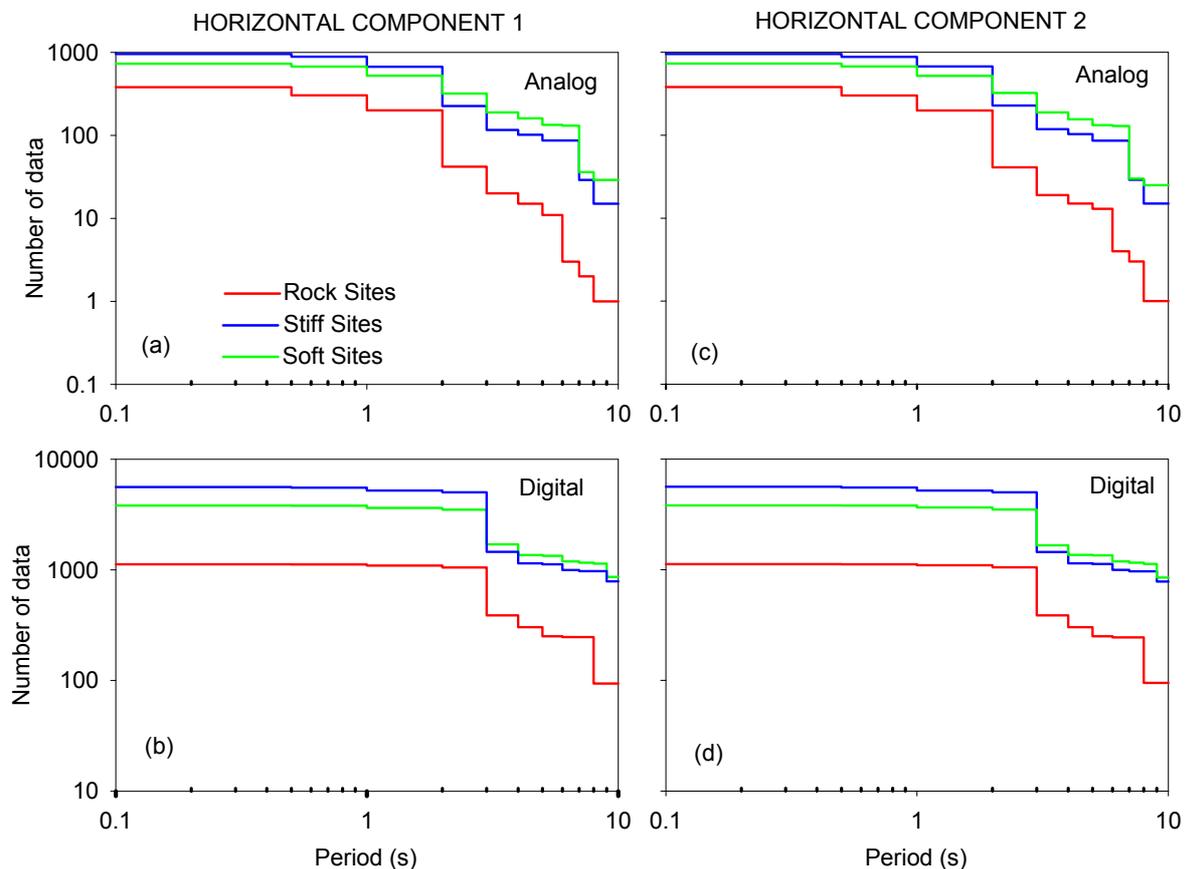
Figure 11. Site-class dependent record numbers as a function of usable period for analog (top row) and digital (bottom row) instruments. The plots for horizontal components are displayed column-wise.

25
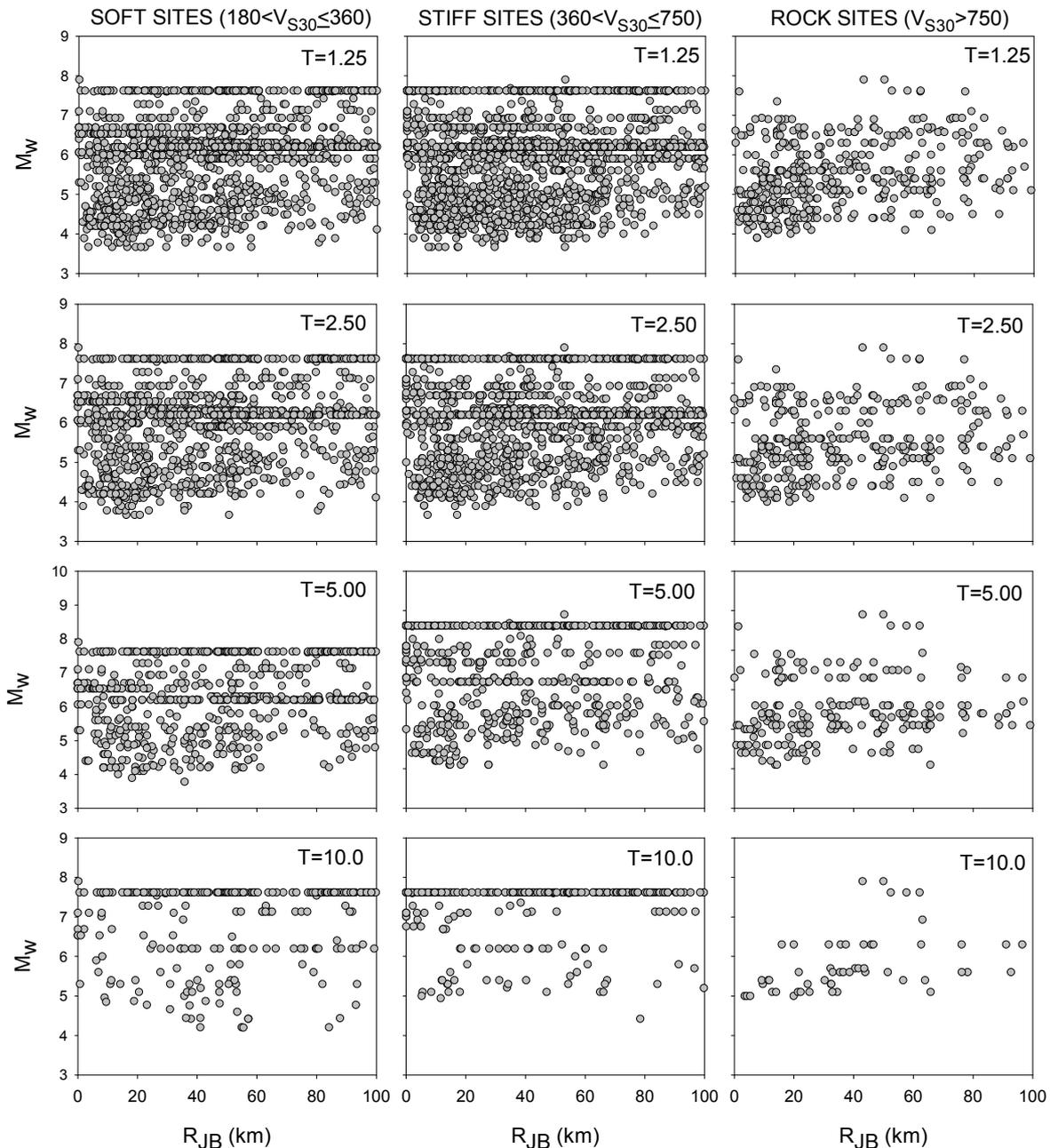
Figure 12 The magnitude-distance-site class scatters of ground motions for soft (left column), stiff (middle column) and rock (right column) sites at different periods.

Observations on the Duplicated Ground Motions

While conducting this study, it is observed that some of the duplicated records reported by different databases show significant variations (differences) in term of PGA. For example, Figure 13 compares the acceleration time histories of Codroipo record from the 15/09/1976 Friuli, Italy aftershock (M_w = 5.9, R_{epi} = 41.1 km). This recording is common in the ISESD, ITACA, and NGA databases. When the first horizontal component of the ground motion is of concern (top row in Figure 13), ITACA and NGA databases provide similar time histories. However, the time history of the same component provided by ISESD includes a spike around 8 seconds. The spike governs and misleads the PGA calculation since its amplitude is larger than the actual peak acceleration value. For the other two components (middle and

26

bottom rows in Figure 13), all databases present similar ground-motion time histories and their PGA values do not differ too much.
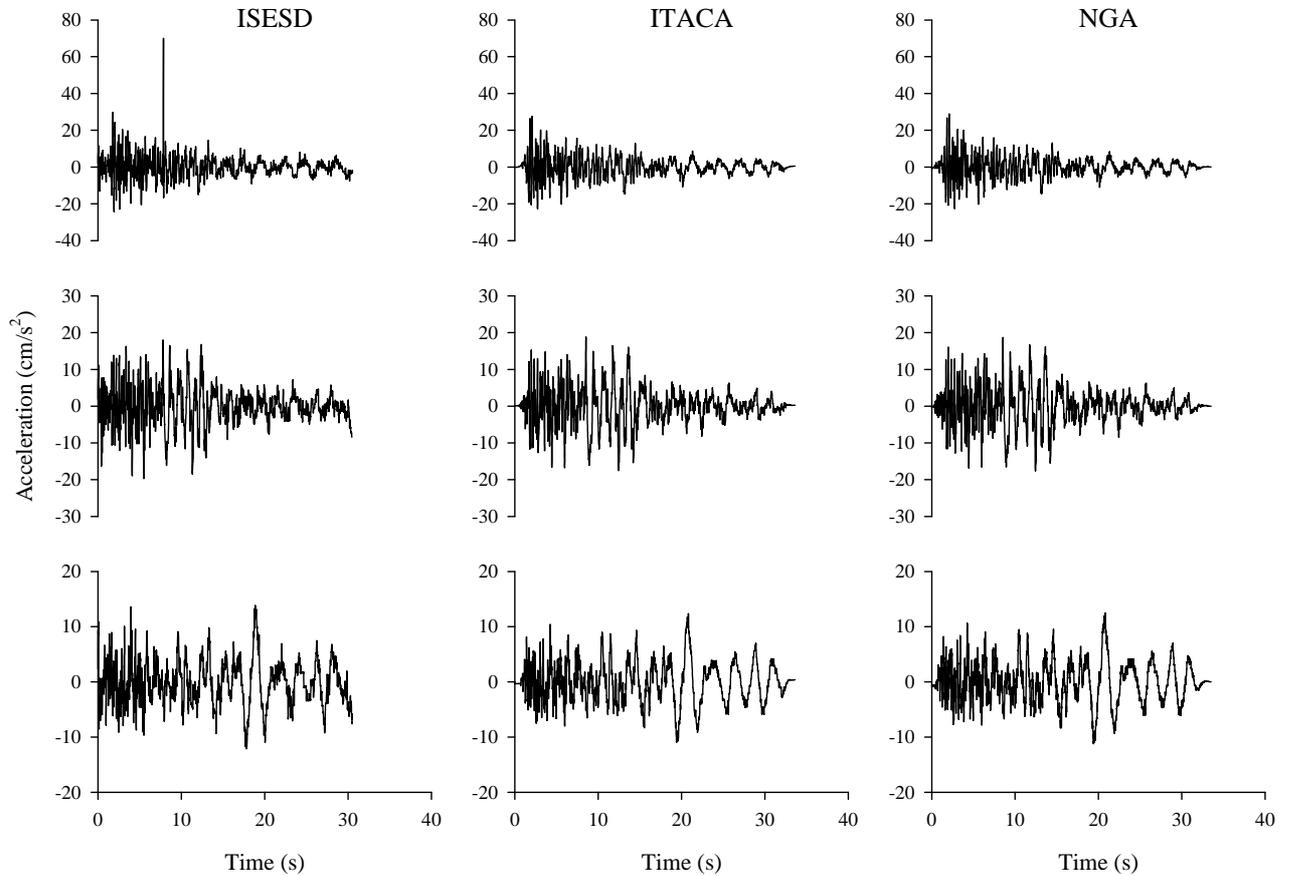
Figure 13. Comparison of the acceleration time histories of Codroipo record (Waveform ID: 161) of 15/09/1976 Friuli/Italy aftershock (Earthquake ID: 55) presented by ISESD (left column), ITACA (middle column) and NGA (right column) databases. The horizontal components of the records are presented in the first two rows. The bottom row displays the vertical components of the records. The vertical axes are kept same for each component for a better visual inspection.

Another comparison for the duplicated acceleration time series is displayed in Figure 14. The left and right columns show the Izmir station record of the 16/12/1977 Izmir, Turkey earthquake (M_w = 5.6, R_{epi} = 2.0 km) provided by the ISSED and NGA databases, respectively. The horizontal acceleration amplitudes of the NGA record are approximately twice larger than that of the ISESD record. Vertical component of NGA record also attains larger accelerations with respect to the ISESD record. Inspection of the processing procedures and selected filter cut-off frequencies revealed that NGA implemented causal Butterworth band-pass filter whereas the ISESD database processed the same accelerogram by the elliptical band-pass filter. The high-cut frequencies used by these two databases are fairly similar with values ranging between 20-25 Hz. However, the selected low-cut frequencies for the horizontal components show significant differences: $f_{low-cut}$ = 0.25 Hz and 1.00 Hz in the ISESD and NGA databases, respectively. Interestingly, larger low-cut filter frequency implemented by the NGA database results in higher accelerations with respect to the ISESD data. This is quite unexpected and it indicates that the differences in data processing schemes may yield larger variations in the amplitudes of the acceleration

time series and PGA values. The observations presented here suggest that some of the duplicated accelerograms may require visual inspection before their use in the SHARE project. However, this is left to the working groups within the project since the suits of ground motions assembled by working groups may differ from each other based on their specific objectives.
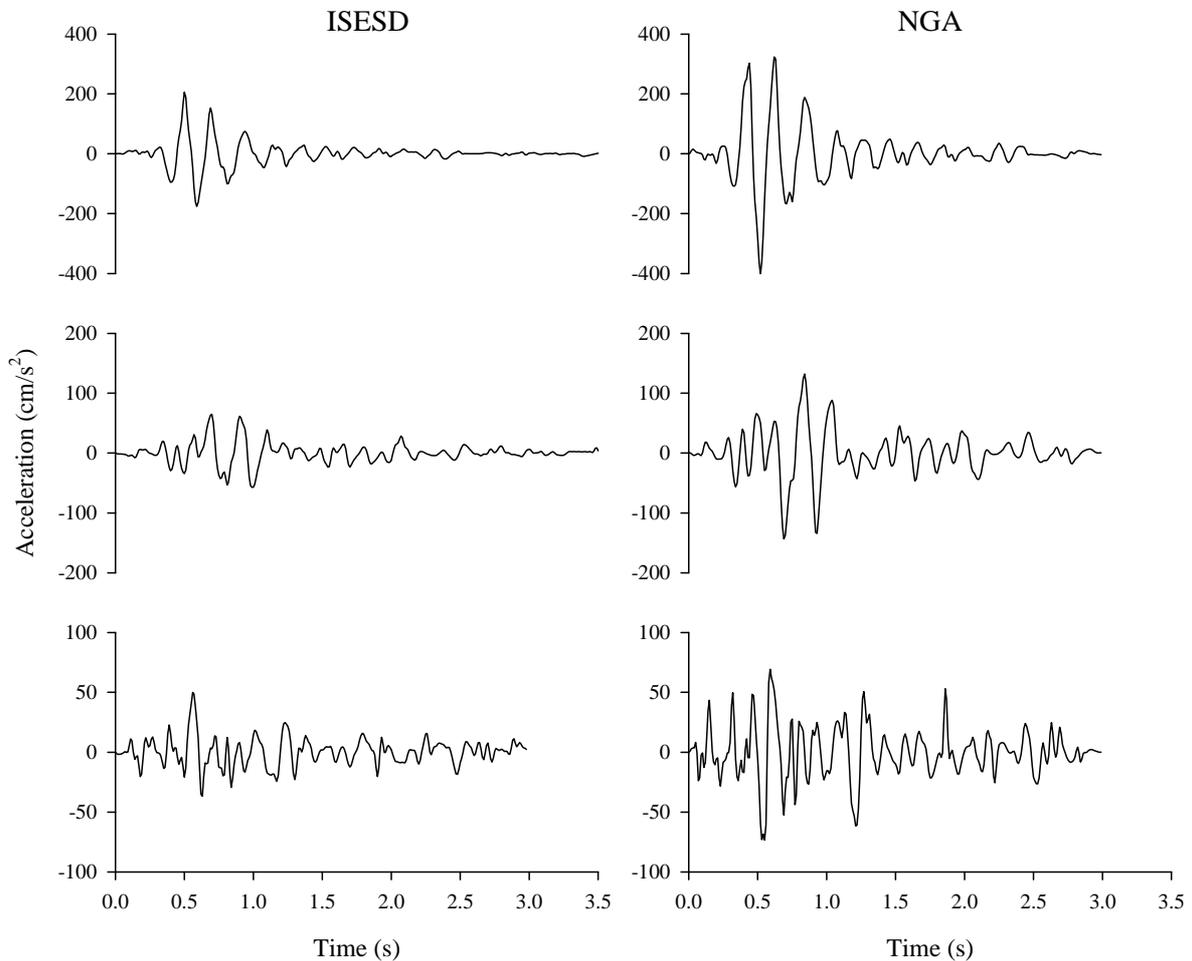
Figure 14. Comparison of the acceleration time series of the Izmir record (Waveform ID: 16359) from the 16/12/1977 Izmir, Turkey earthquake (Earthquake ID: 63). The left column presents the ISESD version of the data and the right column displays the NGA version. The horizontal components of the records are presented in the first two rows. The lower row displays the vertical components of the data.

Summary and Conclusion

Within the scope of "Seismic Hazard Harmonization in Europe" (SHARE) project an extended global worldwide strong ground-motion databank is compiled from seven different databases: Cauzzi and Faccioli database (C&F), the KIK-Net database, the European Strong-Motion Database (ESMD), the Next Generation Attenuation database (NGA), the Turkish National Strong-Motion database (T-NSMP), the Internet Site for European Strong-motion Data (ISESD) database, and Italian Accelerometric Archive (ITACA) database. The outcomes of the recent ITACA and T-NSMP projects are also utilized for updating the site

classes of Italian and Turkish strong-motion sites that exist in the C&F, NGA, ESMD and ISESD databases.

In the first stage of the compilation process, the strong ground-motion databases are individually assessed to identify their main seismological features. Each database is investigated in terms of earthquake and recording station information as well as ground motions. During the evaluation process, the limitations of databases and the observed inconsistencies within the databases are identified. The characteristics of databases are described and the strategies followed in handling the conflicting cases are explained. Examples are presented to demonstrate these inconsistencies and the methodology to handle them.

After removing the inconsistent information in each database, they are unified to form the metadata of the integrated SHARE databank. The unification of databases is performed by transferring all relevant information to the integrated metafile. Then the duplicated earthquakes, stations and records are identified based on the methodology described in the second part of the report.

Finally, the unified databank is described in terms of several seismological parameters to present a general overview about the extents of the databank. The histograms and scatters of earthquakes and ground-motion records covered in the databank are examined in terms of magnitude, depth, faulting style, EC8 site category, various source-to-site distances, filter cut-off frequencies and usable period ranges of ground motions. The major characteristics and constraints of the databank are described according to these seismological parameters. Some methods are proposed for the possible improvements in the databank. Additionally, some observations made on the duplicated ground motions are presented with specific examples.

References

Akkar, S. and Bommer, J.J., (2006). Influence of long-period filter cut-off on elastic spectral displacements, *Earthquake Engineering and Structural Dynamics*, **35**: 1145-1165.

Akkar, S., Cagnan, Z., Yenier, E., Erdogan, E., Sandikkaya, M.A., Gulkan, P., (2010). The recently compiled Turkish strong-motion database: preliminary investigation for seismological parameters, *Journal of Seismology*, 14.

Ambraseys N.N , Douglas J., Sigbjörnsson R., Berge-Thierry C., Suhadolc P., Costa G., Smit P., (2004a). Dissemination of European Strong Motion Data Vol:2 Using Strong Motion Datascape Navigator. CD-ROM collection, Feb. Engineering and Physical Sciences Research Council, United Kingdom.

Ambraseys N.N, Smit P, Douglas J., Margaris B, Sigbjörnsson R., Olafsson S, Suhadolc P, and Costa G (2004b). Internet site for European strong-motion data, *Bollettino di Geofisica Teorica ed Applicata*, **45**: 113-129.

Atkinson, G.M. and Silva, W., (2000). Stochastic Modeling of California Ground Motions, *Bulletin of the Seismological Society of America,* **90**:255–274.

Boore D.M., (2004). Estimating VS(30) (or NEHRP site classes) from shallow velocity models (depths <30 m). *Bulletin of the Seismological Society of America,* **94**(2):591–597.
Boore D.M.,(2005). On pads and filters: Processing strong-motion data, *Bulletin of the Seismological Society of America,* **95**:745–750.

Boore, D.M., Joyner, W.B. and Fumal, T.E., (1997). Equations for estimating horizontal response spectra and peak acceleration from western North American earthquakes: a summary of recent work. *Seismological Research Letters*, **68**: 128-153.

Boore, D.M., Watson-Lamprey, J. and Abrahamson, N.A., (2006). GMRotD and GMRotI: Orientation-independent measures of ground motion, *Bulletin of the Seismological Society of America*, **96**: 1502-1511.

Bray, J.D., and Rodriguez-Marek, A., (1997). Geotechnical site categories proceedings, First PEER-PG&E Workshop on Seismic Reliability of Utility Lifelines, San Francisco, CA, August.

Building Seismic Safety Council (BSSC), (2003). *NEHRP Recommended Provisions for Seismic Regulations for New Buildings and Other Structures*, *FEMA-450,* 2003 revision, Federal Emergency Management Agency, Washington D. C.

Campbell, K.W., (1997). Empirical near-source attenuation relationships for horizontal and vertical components of peak ground acceleration, peak ground velocity, and pseudo-absolute acceleration response spectra, *Seismological Research Letters*, **68**: 154-179.

Campbell, K.W., and Bozorgnia, Y., (2003). Updated near-source ground-motion (attenuation) relations for the horizontal and vertical components of peak ground acceleration and acceleration response spectra, *Bulletin of the Seismological Society of America*, **93**(1), 314–331.

Cauzzi, C. and Faccioli, E. (2008). Broadband (0.05 to 20 s) prediction of displacement response spectra based on worldwide digital records, *Journal of Seismology*, **12**(4): 453-475.

Chiou, B., Darragh, R., Gregor, N. and Silva, W. (2008) NGA Project Strong-Motion Database, *Earthquake Spectra*, **24**(1): 23-44.

Douglas, J., (2003). What is a poor quality strong-motion record?, *Bulletin of Earthquake Engineering*, **1**: 141-156.

European Committee for Standardization, CEN (2003). "Eurocode 8: Design of structures for earthquake resistance - Part 1: General rules, seismic actions and rules for buildings", European Committee for Standardization, Brussels.

Frohlich, C. and Apperson, K.D., (1992). Earthquake focal mechanisms, moment tensors, and the consistency of seismic activity near plate boundaries, *Tectonics*, **11**: 279-296.

ISESD website: http://www.isesd.hi.is/ESD_Local/frameset.htm (last visited 13.11.2009).

ITACA website: http://itaca.mi.ingv.it/ItacaNet (last visited 08.02.2010).

Pousse, G., Thierry, C.B and Bard, P.-Y. (2005). Eurocode 8 Design response spectra evaluation using the K-NET Japanese database, *Journal of Earthquake Engineering*, **9**(4): 547-574.

Sadigh, K., Chang, C.Y., Egan, J. A., Makdisi, F. and Youngs, R.R., (1997). Attenuation relationships for shallow crustal earthquakes based on California strong motion data, *Seismological Research Letters*, **68**: 180-189.

Sandıkkaya, M. A., (2008). *Site classification of Turkish national strong-motion recording sites, M.Sc. Thesis,* Civil Engineering Department, Middle East Technical University, Ankara.

Wells, D.L. and Coppersmith, K.J., (1994). New empirical relationships among magnitude, rupture length, rupture width, rupture area, and surface displacement, *Bulletin of the Seismological Society of America,* **84**: 974-1002.

APPENDIX A

Table A.1 Differences between EC8 site classes computed from available V_{S30} values and those given by C&F database (AGC)

STATION CODE (C&F)	STATION NAME	V_{S30} (m/s)	EC8 Site Category	AGC
NGS002	MATSUURA	176	D	C
YMG002	HAGI	181	C	D
YMG001	SUSA	184	C	D
SMN005	IZUMO	185	C	D
AIC010	TSUKUDE	185	C	D
TYM005	SHINMINATO	186	C	D
MYZ013	MIYAZAKI	188	C	D
NIG010	NIIGATA	204	C	D
KMM016	HITOYOSHI	327	C	B
HKD024	TATSUPU	336	C	B
HRS003	MIYOSHI	338	C	B
SMN003	YOKOTA	339	C	B
YMT012	NAGAI	346	C	B
KGS028	KAMIYAKU	348	C	B
FKS008	FUNEHIKI	349	C	B
FKS009	ONO	350	C	B
KMM015	MINAMATA	351	C	B
HKD176	YOMBANKAWA	351	C	B
OKY014	SHIMOTSUI	352	C	B
NIG024	YASUDUKA	352	C	B
YMT009	SAGAE	353	C	B
HRS001	TAKANO	353	C	B
NGS004	SASEBO	356	C	B
KMM009	YABE	356	C	B
KNG006	FUTAMATAGAWA	357	C	B
KMM013	TANOURA	357	C	B
TYM009	YATSUO	357	C	B
HRS021	SAIJOH	358	C	B
CHB018	KATSUURA	359	C	B
NGS009	ISAHAYA	361	B	C
MYG005	NARUKO	361	B	C
SZO008	NUMADU	363	B	C
TTR006	AKASAKI	364	B	C
YMG009	KANO	368	B	C
SMN013	MASUDA	668	B	A
FKO014	YABE	679	B	A
OIT006	INNAI	721	B	A
MYZ004	MANGOH	736	B	A
IWT010	ICHINOSEKI	744	B	A

STATION CODE (C&F)	STATION NAME	STATION LAT.	STATION LONG.
GNM015	SHIMONITA	744	B	A
HYG004	MURAOKA	764	B	A
NGS008	KONAGAI	770	B	A

Table A.2 Typical examples of inconsistencies observed in the station information of C&F database and corrections made for these inconsistencies. The same stations are grouped and each group is separated by a line. Note that the red colored data are changed in each group.

STATION CODE (C&F)	STATION NAME	STATION LAT.	STATION LONG.
515	Pinyon Flat Observatory	33.607	-116.453
515	CA: Pinyon Flat; UCSD Geophys Obs	33.6076	-116.454
1417	Mentone Fire Station #9	34.07	-117.121
1417*	Adapazari Kadin D	40.773	30.398
AKT022	TAMAGAWA	39.771	140.67
AKT022	TAMAGAWA	39.7711	140.6702
AKT023	TSUBAKIDAI	39.143	140.721
AKT023	TSUBAKIDAI	39.143	140.721
AKT023	TSUBAKIDAI	39.1433	140.7205
FKO006	FUKUOKA	33.5969	130.3985
FKO006	FUKUOKA	33.594	130.401
FKS001	SOHMA	37.792	140.923
FKS001	SOHMA	37.7919	140.923
FKS002	YANAGAWA	37.842	140.605
FKS002	YANAGAWA	37.8419	140.6047
FKS004	IITATE	37.677	140.738
FKS004	IITATE	37.677	140.738
FKS004	IITATE	37.6769	140.738
FKS010	HIRONO	37.231	141.005
FKS010	HIRONO	37.2311	141.005
FKS020	INAWASHIRO	37.544	140.111
FKS020	INAWASHIRO	37.5444	140.1111

*Assigned a new station code "1418"

APPENDIX B

Table B.1 Typical examples of inconsistencies observed in the station information of KIK-Net database and corrections made for these inconsistencies. The same stations are grouped and each group is separated by a line. Note that the red colored data are changed in each group.

STATION CODE (KIK-Net)	STATION LAT.	STATION LONG.	ALTITUDE AT SURFACE (m)	ALTITUDE AT BELOW THE GROUND (m)
KGWH03	34.2669	134.1511	50	-50
KGWH03	34.2668	134.1508	50	-50
KGWH03	34.2668	134.1508	50	-50
KMMH06	32.8081	131.1033	493	382
KMMH06	32.8081	131.1033	492	381
KMMH06	32.8081	131.1033	492	381
KMMH06	32.8081	131.1033	493	382
KMMH06	32.8081	131.1033	493	382
KMMH06	32.8081	131.1033	493	382
KMMH06	32.8081	131.1033	493	382
KMMH06	32.8081	131.1033	493	382
KMMH06	32.8081	131.1033	493	382
KMMH06	32.8081	131.1033	493	382
KMMH06	32.8081	131.1033	492	381
KMMH06	32.8081	131.1033	493	382
KMMH06	32.8081	131.1033	492	381
KMMH06	32.8081	131.1033	492	381
KMMH06	32.8081	131.1033	492	381
KMMH06	32.8081	131.1033	492	381
KMMH06	32.8081	131.1033	492	381
KMMH06	32.8081	131.1033	492	381
KMMH06	32.8081	131.1033	493	382
KMMH06	32.8081	131.1033	493	382
KMMH06	32.8081	131.1033	493	382
KMMH06	32.8081	131.1033	493	382
KMMH06	32.8081	131.1033	493	382
KMMH07	32.62	130.5603	22	-278
KMMH07	32.62	130.5608	22	-278
KMMH07	32.62	130.5603	22	-278
KMMH07	32.62	130.5603	22	-278
KMMH07	32.62	130.5603	22	-278
KMMH07	32.62	130.5603	22	-278
KMMH07	32.62	130.5603	22	-278
KMMH07	32.62	130.5603	22	-278
KMMH07	32.62	130.5603	22	-278
KMMH07	32.62	130.5603	22	-278

KMMH07	32.62	130.5603	22	-278
KMMH07	32.62	130.5608	22	-278
KMMH07	32.62	130.5608	22	-278
KMMH07	32.62	130.5608	22	-278
KMMH07	32.62	130.5608	22	-278
KMMH07	32.62	130.5608	22	-278
KMMH07	32.62	130.5608	22	-278
KMMH07	32.62	130.5608	22	-278
KMMH07	32.62	130.5608	22	-278
KMMH07	32.62	130.5603	22	-278
KMMH07	32.62	130.5603	22	-278
KMMH07	32.62	130.5603	22	-278
OKYH01	34.5036	133.8931	10	-191
OKYH01	34.5036	133.8931	10	-191
OKYH01	34.5037	133.8931	10	-191
OKYH01	34.5037	133.8931	10	-191
OKYH01	34.5036	133.8931	10	-191
OKYH01	34.5036	133.8931	10	-191
OKYH04	34.6397	133.6886	50	-50
OKYH04	34.6397	133.6886	50	-50
OKYH04	34.6397	133.6886	50	-50
OKYH04	34.6397	133.6886	50	-50
OKYH04	34.6397	133.6886	50	-50
OKYH04	34.6397	133.6888	50	-50
OKYH04	34.6397	133.6886	50	-50
OKYH04	34.6397	133.6886	50	-50
OKYH04	34.6397	133.6886	50	-50
TTRH02	35.2281	133.3937	410	310
TTRH02	35.2281	133.3937	410	310
TTRH02	35.2281	133.3937	410	310
TTRH02	35.2281	133.3937	410	310
TTRH02	35.2281	133.3937	410	310
TTRH02	35.2281	133.3937	410	310
TTRH02	35.2281	133.3936	410	310
YMGH12	34.2143	131.3621	150	48
YMGH12	34.2144	131.3619	150	48

APPENDIX C

Table C.1 Inconsistencies between the names of record files and the record names presented in the NGA database

Available Record Names	In Database
LOMAP_HYN064.AT2	Hayward City Hall
LOMAP_HYN334.AT2	Hayward City Hall
LOMAP_MEN270.AT2	Foster City - Menhaden Court
LOMAP_MEN360.AT2	Foster City - Menhaden Court
ANZA\ELS015.AT2	ANZA/ELS-UP.at2
ANZA\ELS105.AT2	ANZA/ELS105.at2

Table C.2 Record files that are provided but not listed in the NGA database

NORTHR\5080-UP.AT2
NORTHR\5229A-UP.AT2
NORTHR\5229-UP.AT2

Table C.3 List of names of the record files that are not provided but listed in the NGA database

BORAH.AS\BORXXX	MAMMOTH\C-XMGXXX	PALMSPR\CLJXXX
BORAH.AS\CEMXXX	MAMMOTH\H-XMMXXX	PALMSPR\DSPXXX
BORAH.AS\HAUXXX	MORGAN\A1EXXX	PALMSPR\PSAXXX
BORAH.MS\CPPAXXX	MORGAN\WNEXXX	ROERMOND\GSHXXX
BORAH.MS\CPPBXXX	MORGAN\WSEXXX	SFERN\C08XXX
BORAH.MS\PBFXXX	MORGAN\WVEXXX	SFERN\PDLXXX
BORAH.MS\TANXXX	NAHANNI\S2XXX	SMART1\25C0XXX
CHICHI\HWA054XX	NCALIF\D-SCAXXX	SUPERST\B-BRAXXX
CHICHI\TTN047XX	NCALIF\D-SCPXXX	SUPERST\B-CALXXX
COALINGA\A-YUBXXX	NORTH392\HOWXXX	SUPERST\B-KRNXXX
COALINGA\H-PGDXXX	NORTH392\KATXXX	SUPERST\B-PLSXXX
HOLLISTR\A-G01XXX	NORTH392\MCSXXX	SUPERST\B-POEXXX
KOZANI\B-GR1XXX	NORTH392\MU2XXX	SUPERST\B-PTSXXX
KOZANI\C-GRPXXX	NORTH392\WILXXX	SUPERST\B-SUPXXX
KOZANI\EDEXXX	NORTHR\GARXXX	SUPERST\B-WLFXXX
LOMAP\SPGXXX	NORTHR\STCXXX	WHITTIER\A-L01XXX
LOMAP\WVCXXX	OROVILLE\A-ORVXXX	WHITTIER\A-MANXXX
LYTLECR\CSMXXX		

Table C.4 List of the available records that have only header information without the acceleration time series

BEARCTY\0551c_H1xxx.AT2	MAMMOTH\D-HCF_H1XXX.at2
BIGBEAR\SB2-H1xxx.AT2	MAMMOTH\D-HCF_H2XXX.at2
CHICHI\HWA053-H1XXX.AT2	MANJIL\190-H2xxx.AT2
COALINGA\A-MIT-H2xxx.AT2	MORGAN\WNE-H2xxx.AT2
COALINGA\H-PGD-h2xxx.AT2	MORGAN\WSE-H2xxx.AT2
COALINGA\H-VC5-H2xxx.AT2	MORGAN\WVE-H2xxx.AT2
HECTOR\0535a_H2xxx.AT2	NWCHINA3\X411N-H2xxx.AT2
HOLLISTR\D-HD4-H2xxx.AT2	PARKF\C02-H2xxx.AT2
IMPVALL\H-E02_H2xxx.AT2	VICT\QKP-H2xxx.AT2
IMPVALL\H-QKP-H2xxx.AT2	WHITTIER\A-FLO-H2xxx.AT2
KOCAELI\SKR-H1XXX.AT2	WHITTIER\A-MAN-H2xxx.AT2
LOMAP\SPG-H2xxx.AT2	

APPENDIX D

Table D.1. Conflicting Italian strong-motion site classes between ITACA and C&F

STATION NAME	ESTIMATED SITE CLASS BY ITACA	V_{S30} (m/s) and SITE CLASS BY C&F
Rieti (Cab. Enel)	C	170, D
Arienzo	A	912, A
Colfiorito Casermette	C	No V_{S30}, A
Nocera Umbra Biscontini	C	No V_{S30}, A
Annifo	C	No information
Cesi Monte	A	No information

A: V_{S30} > 800 m/s, B: 360 m/s ≤ V_{S30} ≤ 800 m/s, C: 180 m/s ≤ V_{S30} < 360 m/s and D: V_{S30} < 180 m/s. Note that EC8 E is a special site category where the soil profile consists of a surface alluvium layer with V_S values of EC8 C or D and thickness varying between about 5-20 m, underlain by stiffer material with V_S>800 m/s.

Table D.2. Conflicting Italian strong-motion site classes between ITACA and NGA

STATION NAME	V_{S30} (m/s) and ESTIMATED SITE CLASS BY ITACA	V_{S30} (m/s) and SITE CLASS BY NGA
Bovino	364.6, C	274.5, C
Mercato S. Severino	483.2, B	350, C
Pontecorvo	No V_{S30}, A	338.6, C
Tolmezzo - Diga Ambiesta 1	No V_{S30}, A	424.8, B
Barcis	No V_{S30}, A	424.8, B
Feltre	No V_{S30}, A	659.6, B
S. Rocco	No V_{S30}, A	659.6, B
Cascia	No V_{S30}, A	659.6, B
Torre Del Greco	No V_{S30}, A	659.6, B
Atina	No V_{S30}, A	659.6, B
Codroipo	No V_{S30}, B	274.5, C
Conegliano Veneto	No V_{S30}, B	274.5, C
S. Agapito	No V_{S30}, B	338.6, C
Bevagna	No V_{S30}, C	1000, A

For EC8 site class definitions, see the footnote given in Table D.1.

Table D.3. Conflicting Italian strong-motion site classes between ITACA and ESMD

STATION NAME	V_{S30} (m/s) and ESTIMATED SITE CLASS BY ITACA	V_{S30} (m/s) and SITE CLASS BY ESMD
Colfiorito	142.6, D	No V_{S30}, B
Garigliano - Free Field 1	192, C	180, C
Garigliano - Free Field 2	192, C	180, C
Bovino	364.6, B	346, C
Tarcento	708.1, B	847, A

S. Rocco	No V_{S30}, A	600, B
Naso	No V_{S30}, A	No V_{S30}, B
Nocera Umbra Salmata	No V_{S30}, A	No V_{S30}, C
Sellano Ovest	No V_{S30}, B	No V_{S30}, A
Rieti (Cab. Enel)	No V_{S30}, C	170, D
Maiano	No V_{S30}, C	367, B
Lioni - Macello	No V_{S30}, C	No V_{S30}, A
Roccamonfina	No V_{S30}, C	No V_{S30}, A
Colfiorito Casermette	No V_{S30}, C	No V_{S30}, A
Nocera Umbra Biscontini	No V_{S30}, C	No V_{S30}, A
Spoleto	No V_{S30}, C	No V_{S30}, B
Bevagna	No V_{S30}, C	No V_{S30}, B
Procisa Nuova	No V_{S30}, C	No V_{S30}, B
Matelica	No V_{S30}, C	No V_{S30}, B
Bussi	No V_{S30}, E	No V_{S30}, A
Nocera Umbra	No V_{S30}, E	No V_{S30}, A
Nocera Umbra 2	No V_{S30}, E	No V_{S30}, A
Milazzo	No V_{S30}, E	No V_{S30}, A

For EC8 site class definitions, see the footnote given in Table D.1.

Table D.4. Conflicting Italian strong-motion site classes between ITACA and ISESD

STATION NAME	V_{S30} (m/s) and ESTIMATED SITE CLASS BY ITACA	V_{S30} (m/s) and SITE CLASS BY ISESD
Colfiorito	142.6, D	221, C
Garigliano - Free Field 1	192, C	180, C
Garigliano - Free Field 2	192, C	180, C
Città Di Castello	285.7, C	No information
Bovino	364.6, B	346, C
Ancona - Palombina	549.1, B	No information
Ancona - Rocca	549.1, B	No information
Norcia	681.2, B	No information
Tarcento	708.1, B	847, A
S. Rocco	No V_{S30}, A	600, B
Rieti (Cab. Enel)	No V_{S30}, C	170, D
Maiano	No V_{S30}, C	367, B
Gubbio Piana	No V_{S30}, C	450, B
Cairano 2	No V_{S30}, C	625, B
Nocera Umbra	No V_{S30}, E	546, B
Nocera Umbra 2	No V_{S30}, E	546, B
Feltre	No V_{S30}, A	No information
Tregnago	No V_{S30}, A	No information
Asiago (Roana)	No V_{S30}, A	No information
Barcis	No V_{S30}, A	No information
Cascia	No V_{S30}, A	No information

Torre Del Greco	No V_{S30}, A	No information
Pontecorvo	No V_{S30}, A	No information
Atina	No V_{S30}, A	No information
Assisi	No V_{S30}, A	No information
Nocera Umbra Salmata	No V_{S30}, A	No information
Gubbio	No V_{S30}, A	No information
Cassignano	No V_{S30}, A	No information
Ferruzzano (Africo Nuovo)	No V_{S30}, A	No information
Naso	No V_{S30}, A	No information
Messina 1	No V_{S30}, A	No information
Atina - Pretura Piano Terra	No V_{S30}, A	No information
Atina - Pretura Terrazza	No V_{S30}, A	No information
Villetta Barrea	No V_{S30}, A	No information
Monte Fiegni (Fiastra)	No V_{S30}, A	No information
Umbertide	No V_{S30}, A	No information
Pietralunga	No V_{S30}, A	No information
Peglio	No V_{S30}, A	No information
Pennabilli	No V_{S30}, A	No information
Malcesine	No V_{S30}, A	No information
Arquata Del Tronto	No V_{S30}, A	No information
Cascia - Petrucci	No V_{S30}, A	No information
S. Vittorino (L Aquila)	No V_{S30}, A	No information
Spoleto (Monteluco)	No V_{S30}, A	No information
Mascioni (Campotosto)	No V_{S30}, A	No information
Vagli - Paese	No V_{S30}, A	No information
Barga	No V_{S30}, A	No information
Lauria	No V_{S30}, A	No information
S. Giorgio La Molara	No V_{S30}, A	No information
Cagli	No V_{S30}, A	No information
Ripa (Fagnano)	No V_{S30}, A	No information
Pescasseroli	No V_{S30}, A	No information
Atina - Pretura Esterno	No V_{S30}, A	No information
Forca Canapine (Arquata Tronto)	No V_{S30}, A	No information
Serravalle Di Chienti	No V_{S30}, A	No information
L Aquila - V. Aterno - Colle Grilli	No V_{S30}, A	No information
Scafa	No V_{S30}, A	No information
Pistoia	No V_{S30}, A	No information
Sestola	No V_{S30}, A	No information
Giarre	No V_{S30}, A	No information
Sortino	No V_{S30}, A	No information
Vizzini	No V_{S30}, A	No information
Noto	No V_{S30}, A	No information
Pachino	No V_{S30}, A	No information
Taranta Peligna	No V_{S30}, A	No information
Codroipo	No V_{S30}, B	No information

Conegliano Veneto	No V_{S30}, B	No information
Teora - Contrada Fiumicello	No V_{S30}, B	No information
S. Agapito	No V_{S30}, B	No information
Sellano Ovest	No V_{S30}, B	No information
Castelfranco Veneto	No V_{S30}, B	No information
Cortina D Ampezzo	No V_{S30}, B	No information
Castelnuovo (San Pio)	No V_{S30}, B	No information
Poggio Picenze	No V_{S30}, B	No information
Barisciano	No V_{S30}, B	No information
Senigallia	No V_{S30}, B	No information
L Aquila - V. Aterno - Aquil Park Ing.	No V_{S30}, B	No information
L Aquila - V. Aterno - Aquil Park Int.	No V_{S30}, B	No information
Cosenza	No V_{S30}, B	No information
Mazara Del Vallo	No V_{S30}, B	No information
Lauria Galdo	No V_{S30}, B	No information
Roggiano Gravina	No V_{S30}, B	No information
Fornovo	No V_{S30}, B	No information
Villa San Giovanni - 2	No V_{S30}, B	No information
Spoleto	No V_{S30}, C	No information
Bevagna	No V_{S30}, C	No information
Procisa Nuova	No V_{S30}, C	No information
Lioni - Macello	No V_{S30}, C	No information
Roccamonfina	No V_{S30}, C	No information
Cassino - Sant Elia	No V_{S30}, C	No information
Colfiorito Casermette	No V_{S30}, C	No information
Nocera Umbra Biscontini	No V_{S30}, C	No information
Castelnuovo (Assisi)	No V_{S30}, C	No information
Pellaro (Cab. Enel)	No V_{S30}, C	No information
Patti	No V_{S30}, C	No information
Borgo Ottomila - 2 (Celano)	No V_{S30}, C	No information
Monselice	No V_{S30}, C	No information
Salsominore	No V_{S30}, C	No information
Ortucchio	No V_{S30}, C	No information
Leonessa	No V_{S30}, C	No information
Pinerolo	No V_{S30}, C	No information
Novellara	No V_{S30}, C	No information
Sorbolo	No V_{S30}, C	No information
Gioia Sannitica	No V_{S30}, C	No information
Vagli Centrale - Base Diga 1	No V_{S30}, C	No information
Bussi	No V_{S30}, E	No information
Milazzo	No V_{S30}, E	No information

For EC8 site class definitions, see the footnote given in Table D.1.

Table D.5. Conflicting Turkish strong-motion site classes between T-NSMP and C&F

STATION NAME	V_{S30} (m/s) and SITE CLASS BY T-NSMP	V_{S30} (m/s) and SITE CLASS BY C&F
Sakarya Karadere Koyu (LDEO- VO)	481.3, B	No V_{S30}, A
Bingol Merkez Bayindirlik Ve Iskan Mudurlugu	528.7, B	806, A

For EC8 site class definitions, see the footnote given in Table D.1.

Table D.6. Conflicting Turkish strong-motion site classes between T-NSMP and NGA

STATION NAME	V_{S30} (m/s) and SITE CLASS BY T-NSMP	V_{S30} (m/s) and SITE CLASS BY NGA
Afyon Merkez Bayindirlik Ve Iskan Mudurlugu	225.6, C	No information
Aydin Merkez Tarim Ve Koy Isleri Bakanligi Hayvan Sagligi Sube Mudurlugu	310.9, C	No information
Tokat Merkez Devlet Su Isleri 72. Sube Mudurlugu	323.8, C	No information
Tekirdag Marmara Ereglisi Kaymakamlik Binasi	325.2, C	659.6, B
Manisa Merkez Bayindirlik Ve Iskan Mudurlugu	340.3, C	659.6, B
Bolu Goynuk Goynuk Devlet Hastanesi	347.7, C	424.8, B
Bolu Mudurnu Ptt Binasi	355.4, C	659.6, B
Kastamonu Tosya Meteoroloji Istasyon Mudurlugu	361.8, B	-
Denizli Cardak Cardak Saglik Ocagi	395.1, B	338.6, C
Balikesir Merkez Balikesir Huzurevi	662.0, B	338.6, C
Erzincan Merkez Meteoroloji Mudurlugu	No information	274.5, C
Balikesir Merkez Bayindirlik Ve Iskan Mudurlugu Lojmanlari	No information	338.6, C
Bursa Merkez Bayindirlik Ve Iskan Mudurlugu	No information	338.6, C

For EC8 site class definitions, see the footnote given in Table D.1.

Table D.7 Conflicting Turkish strong-motion site classes between T-NSMP and ESMD

STATION NAME	V_{S30} (m/s) and SITE CLASS BY T-NSMP	V_{S30} (m/s) and SITE CLASS BY ESMD
Usak Merkez Meteoroloji Istasyon Mudurlugu	285.5, C	No V_{S30}, B
Erzurum Horasan Meteoroloji Istasyon Mudurlugu	316.4, C	No V_{S30}, B
Tokat Merkez Devlet Su Isleri 72. Sube Mudurlugu	323.8, C	No V_{S30}, A
Manisa Merkez Bayindirlik Ve Iskan Mudurlugu	340.3, C	No V_{S30}, B
Bolu Goynuk Goynuk Devlet Hastanesi	347.7, C	No V_{S30}, B
Denizli Merkez Bayindirlik Ve Iskan Mudurlugu	355.9, C	No V_{S30}, B
Sakarya Karadere Koyu (LDEO- VO)	481.3, B	No V_{S30}, A
Kocaeli Gebze Tubitak Marmara Arastirma Merkezi	701.1, B	912, A
Erzincan Merkez Meteoroloji Mudurlugu	No information	421, B
Adiyaman Golbasi Golbasi Devlet Hastanesi	No information	No V_{S30}, A

For EC8 site class definitions, see the footnote given in Table D.1.

Table D.8. Conflicting Turkish strong-motion site classes between T-NSMP and ISESD

STATION NAME	V_{S30} (m/s) and SITE CLASS BY T-NSMP	V_{S30} (m/s) and SITE CLASS BY ISESD
Afyon Merkez Bayindirlik Ve Iskan Mudurlugu	225.6, C	No information
Aydin Kosk Kosk Saglik Ocagi	366.9, B	No information
Aydin Kusadasi Meteoroloji Mudurlugu	369.3, B	No information
Aydin Merkez Tarim Ve Koy Isleri Bakanligi Hayvan Sagligi Sube Mudurlugu	310.9, C	No information
Aydin Nazilli Meteoroloji Mudurlugu	267.4, C	No information
Aydin Sultanhisar Meteoroloji Mudurlugu	354.8, C	No information
Balikesir Bandirma Meteoroloji Mudurlugu	321.0, C	No information
Balikesir Dursunbey Kandilli Gozlem Istasyonu	495.9, B	No information
Balikesir Edincik Kandilli Gozlem Istasyonu	520.1, B	No information
Balikesir Edremit Meteoroloji Istasyon Mudurlugu	223.3, C	No information
Balikesir Gonen Meteoroloji Istasyon Mudurlugu	397.2, B	No information
Balikesir Merkez Balikesir Huzurevi	662.0, B	No information
Bingol Merkez Bayindirlik Ve Iskan Mudurlugu	528.7, B	806, B
Bolu Goynuk Goynuk Devlet Hastanesi	347.7, C	No information
Bolu Mudurnu Ptt Binasi	355.4, C	No information
Burdur Bucak Kandilli Gozlem Istasyonu	713.7, B	No information
Burdur Merkez Bayindirlik Ve Iskan Mudurlugu	294.1, C	No information
Burdur Merkez Meteoroloji Istasyon Mudurlugu	334.6, C	No information
Bursa Gemlik Engurucuk Askeri Veteriner Okulu	176.3, D	570, B
Bursa Gemlik Umurbey Saglik Meslek Lisesi	366.2, B	299, C
Bursa Merkez Afet Yonetim Merkezi	249.1, C	No information
Bursa Merkez Sivil Savunma Mudurlugu	456.6, B	No information
Bursa Orhangazi Cargil Tarim Sanayi	348.7, C	462, B
Canakkale Merkez Meteoroloji Istasyon Mudurlugu	191.9, C	No information
Denizli Cardak Cardak Saglik Ocagi	395.1, B	No information
Denizli Merkez Bayindirlik Ve Iskan Mudurlugu	355.9, C	No information
Denizli Merkez Meteoroloji Mudurlugu	345.9, C	No information
Denizli Saraykoy Saraykoy Jeotermal Lojmanlari	232.9, C	No information
Elazig Merkez Bayindirlik Ve Iskan Mudurlugu	407.3, B	No information
Erzincan Merkez Bayindirlik Ve Iskan Mudurlugu	314.2, C	No information
Erzincan Merkez Meteoroloji Mudurlugu	No information	421, B
Erzincan Refahiye Hukumet Konagi	433.1, B	No information
Erzincan Tercan Meteoroloji Mudurlugu	319.6, C	No information
Erzincan Tercan Ptt Binasi	416.7, B	No information
Erzurum Horasan Meteoroloji Istasyon Mudurlugu	316.4, C	No information
Erzurum Merkez Bayindirlik Ve Iskan Mudurlugu	374.9, B	No information
Hatay Merkez Bayindirlik Ve Iskan Mudurlugu	469.5, B	No information
Istanbul K.Cekmece Nukleer Santral Binasi	283.3, C	382, B
Istanbul Merkez Bayindirlik Ve Iskan Mudurlugu	595.2, B	No information
Izmir Bornova Ege Universitesi Ziraat Fakultesi	269.9, C	No information

Kahramanmaras Andirin Tufan Pasa Ilkogretim Okulu	610.8, B	No information
Kahramanmaras Elbistan Meteoroloji Istasyon Mudurlugu	314.9, C	No information
Kahramanmaras Merkez Bayindirlik Ve Iskan Mudurlugu	466.2, B	No information
Kastamonu Tosya Meteoroloji Istasyon Mudurlugu	361.8, B	No information
Kocaeli Gebze Tubitak Marmara Arastirma Merkezi	701.1, B	912, A
Kutahya Merkez Sivil Savunma Mudurlugu	242.5, C	No information
Malatya Dogansehir Meteoroloji Istasyon Mudurlugu	654.4, B	No information
Malatya Merkez Bayindirlik Ve Iskan Mudurlugu	480.8, B	No information
Manisa Merkez Bayindirlik Ve Iskan Mudurlugu	340.3, C	No information
Mugla Bodrum Meteoroloji Istasyon Mudurlugu	746.9, B	No information
Mugla Koycegiz Meteoroloji Istasyon Mudurlugu	371.9, C	No information
Mugla Marmaris Meteoroloji Istasyon Mudurlugu	392.5, B	No information
Sakarya Akyazi Orman Isletme Mudurlugu	271.6, C	No information
Sakarya Karadere Koyu (LDEO- FP)	439.5, B	No information
Sakarya Karadere Koyu (LDEO- VO)	481.3, B	No information
Tekirdag Marmara Ereglisi Kaymakamlik Binasi	325.2, C	No information
Tekirdag Merkez Valilik Binasi	408.7, B	No information
Tokat Merkez Devlet Su Isleri 72. Sube Mudurlugu	323.8, C	No information
Usak Merkez Meteoroloji Istasyon Mudurlugu	285.5, C	No information
Van Merkez Bayindirlik Ve Iskan Mudurlugu	363.1, B	No information

For EC8 site class definitions, see the footnote given in Table D.1.